The Impact of Land-Ocean Contrast on The Seasonal To Decadal Variability of The Northern Hemisphere Jet Stream

Samantha Hallam (samantha.hallam@mu.ie)
Maynooth University: National University of Ireland Maynooth https://orcid.org/0000-0003-3418-2554
Simon Josey
National Oceanography Centre
Gerard McCarthy
Maynooth University: National University of Ireland Maynooth
Joel Hirschi
National Oceanography Centre

Research Article

Keywords: Northern Hemisphere Jet Stream, Ocean-atmosphere interactions, Decadal trends, Seasonal to interannual Jet Stream variability, Twentieth Century Reanalysis.

Posted Date: July 19th, 2021

DOI: https://doi.org/10.21203/rs.3.rs-607067/v1

The impact of land – ocean contrast on the seasonal to decadal variability of the Northern Hemisphere jet stream

Samantha Hallam[1,2,3], Simon A. Josey[1], Gerard McCarthy[2] and Joël Hirschi[1]

[1]National Oceanography Centre, European Way, Southampton, SO14 3ZH, UK.
[2]Irish Climate Analysis Research Units, Maynooth University, Ireland (samantha.hallam@mu.ie)
[3] University of Southampton, National Oceanography Centre, European Way, Southampton, SO14 3ZH, UK.

Abstract

Seasonal to decadal variations in Northern Hemisphere jet stream latitude and speed over land (Eurasia, North America) and oceanic (North Atlantic, North Pacific) regions are presented for the period 1871 – 2011 from the Twentieth Century Reanalysis dataset.

Significant regional differences are seen on seasonal to decadal timescales. The ocean acts to reduce the seasonal jet latitude range from 20° over Eurasia to 10° over the North Atlantic where the ocean meridional heat transport is greatest. The mean jet latitude range is at a minimum in winter (DJF), along the western boundary of the North Pacific and North Atlantic, where the land-sea contrast and SST gradients are strongest. The 141-year trends in jet latitude and speed show differences on a regional basis. The North Atlantic has significant increasing jet latitude trends in all seasons, up to 3° in winter. Eurasia has significant increasing trends in winter and summer, however, no increase is seen across the North Pacific or North America. Jet speed shows significant increases evident in winter (up to 4.7ms^{-1}), spring and autumn over the North Atlantic, Eurasia and North America however, over the North Pacific no increase is observed.

Long term trends are generally overlaid by multidecadal variability, particularly evident in the North Pacific, where 20-year variability in jet latitude and jet speed are seen, associated with the Pacific Decadal Oscillation which explains 50% of the winter variance in jet latitude since 1940.

Northern hemisphere jet variability and trends differ on a regional basis (North Atlantic, North Pacific, Eurasia and America) on seasonal to decadal timescales, indicating different mechanisms are influencing the jet latitude and speed. It is important that the differing regional trends and mechanisms are incorporated into climate models and predictions.

Key words: Northern Hemisphere Jet Stream, Ocean-atmosphere interactions, Decadal trends, Seasonal to interannual Jet Stream variability, Twentieth Century Reanalysis.

1. Introduction

Jet streams are fast, narrow air bands, which flow around the globe in both hemispheres near the tropopause at around 10,000m (Archer and Caldeira, 2008). The flow is predominantly zonal from west to east and results from the equator to pole temperature gradient at the tropopause, and the Coriolis force. Jet speeds reach 45 -70ms^{-1} and possibly higher in winter (Barry and Chorley, 2009). Globally there are two main jets; the polar front jet, which forms along the polar front in the region where there is a sharp temperature contrast between polar and subtropical air (Holton, 1992), and the subtropical jet, which forms on the poleward side of the Hadley cell due to the sharp temperature gradients between the Hadley and Ferrel cells, and also angular momentum (Pena-Ortiz et al., 2013).

Jet stream variations have a significant impact on storm activity and temperature patterns across the northern hemisphere, and accordingly impact the environment and society. Jet streams and their seasonal to decadal variability form an important part of natural climate variability due to their influence on the mid latitude storm tracks (Hurrell, 1995), which form in the region ahead of an upper level trough where reduced cyclonic vorticity causes divergence, favouring surface convergence, cyclonic circulation and storm track formation (Barry and Chorley, 2009). In winter, storm tracks bring heat and moisture to regions that would otherwise be cooler and drier. They can also cause extreme weather events, which have a significant impact on society (Trenberth and Hurrell, 1994). Jet stream variability is therefore an important component of climate 'noise' and understanding the seasonal to decadal variability can help inform the study of what climate change will look like on a regional basis e.g. Ronalds et al. (2018) and Barnes and Simpson (2017).

Long term jet stream changes are potential indicators of a changing climate (Pena-Ortiz et al., 2013). Hartmann et al. (2013) found evidence for a poleward shift in the jet stream and storm tracks since the 1970s, but there are significant differences between studies on the magnitude of the migration and changes in jet velocities. Archer and Caldeira (2008) found a poleward migration in the jet stream of 0.17- 0.19° per decade using NCEP-NCAR reanalysis data from 1958-2007, whilst Fu and Lin (2011) suggest a poleward shift of 1° ± 0.3° between 1979 to 2009. Pena-Ortiz et al. (2013), however, found the winter NHJ had moved poleward by 0.02° to 0.13°/decade using NCEP/NCAR (1979-2008) and the 20th Century Reanalysis (1958-2008) datasets. Woollings et al. (2014) found a poleward shift of the North Atlantic Jet (0-60°W) of 0.2°/ decade using the 20th Century Reanalysis dataset covering the period from 1871-2008. In terms of jet speed, Strong and Davis (2007) found increases up to 15% in the NHJ mean speed between 1958-2007, whilst Archer and Caldeira (2008) found a decrease of -0.2 ms^{-1}/decade.

The variety of results obtained are likely to be caused by differing methodologies used to define the jet streams, dataset used, geographical area studied, and the differing time periods. Furthermore, most of the above studies are of the recent past (1958 onwards) and only Woollings et al. (2014) looked at data from 1871 but only for the North Atlantic. A key motivation for the work here is to study the whole northern hemisphere, for the longest available time period from 1871, using a consistent methodology and dataset.

The global studies outlined do not specifically identify any jet stream trends over oceanic areas compared to land masses despite research which suggests western boundary currents (WBC), through deep atmospheric convection, can influence the entire troposphere on interannual and decadal time-scales (Sheldon and Czaja, 2014, Czaja and Blunt, 2011). The significant sea surface temperature (SST) gradients found along ocean fronts provide an environment for differential sensible and latent heating, which enhances baroclinicity, and leads to surface cyclonic wind convergence and effectively 'anchors' the storm track (Nakamura et al., 2004, Minobe et al., 2008). The sensible heating occurs mainly where cold air from the continents flows over the warm waters (Hoskins and Valdes, 1989). Small et al. (2014) also found that the storm track response to ocean fronts extended into the deep troposphere.

For example, O'Reilly and Czaja (2015) highlight that the changes in the jet stream and storm track over the western Pacific are linked to variations in the Kuroshio Extension Front. When the surface SST gradient was strong the storm track was zonally localised, but there was less influence on the storm track location when the SST gradient was weaker in the 19-year period analysed. In addition, Gan and Wu (2013) found in the North Pacific that cold SST anomalies, typically -0.6°C, north of 30° in autumn led to an increase in baroclinicity and poleward intensification of the storm track in early winter.

In the North Atlantic, Feliks et al. (2016), (2011) have shown that strong SST gradients along mid latitude ocean fronts have a significant influence on the jet stream diffluence angle and low frequency variability. O'Reilly et al. (2016) identified that the Gulf Stream SST front was important in the development of the storm track over the North Atlantic and also influenced European blocking development. Gan and Wu (2014) found that SST anomalies in November and December can influence storm tracks in the following March.

In addition, Woollings et al. (2015) and Fang and Yang (2016) found that cold subpolar SST anomalies influence the atmosphere by strengthening the meridional temperature gradient and baroclinity leading to intensification of the westerly jet stream, in the Atlantic and North Pacific, respectively.

As oceanic influences on the jet stream are now increasingly considered to be important (Simpson et al., 2019) an additional motivation for this study was to look at seasonal to decadal northern hemisphere jet stream variability, and the differences over ocean basins compared to land masses in terms of patterns of variability and long term trends. Accordingly, the northern hemisphere jet stream is analysed over 4 regions; North Atlantic (60°W-0°W), Eurasia (0-120°E), North Pacific (120°E-120°W) and North America (120°W-60°W). Only the northern hemisphere is included in view of the more significant land mass to provide a comparison to the ocean basins and to manage the scope of the study. Pena-Ortiz et al. (2013), Manney and Hegglin (2018) and Spensberger and Spengler (2020) also highlighted that understanding jet stream trends on a regional basis was important.

A regional (land/ocean) jet stream analysis, using a consistent methodology and a long dataset has not been undertaken yet and will provide a broader understanding of the natural variability and decadal trends in the jet stream, essential for validation of climate models (Iqbal et al., 2018, Barnes and Simpson, 2017). Alongside this, the regional longer-term trends in jet latitude and speed will either confirm or challenge studies, which are based on shorter timescales.

2. Data

To understand the jet stream variability the Twentieth Century Reanalysis (V2) (20CR) is used, covering the period from 1871 to 2011. 20CR is based on an ensemble method, with 56 ensemble members, which provides uncertainty estimates on the results obtained. The 20CR fields used here are: air temperature, wind velocities and geopotential height.

20CR is a global atmospheric circulation reanalysis dataset, which assimilates only surface pressure observations and uses an ensemble Kalman Filter data assimilation method and one global numerical weather prediction model (Compo et al., 2006, Compo et al., 2011). Compo et al. (2006), Whitaker et al. (2004), and Anderson et al. (2005) have all shown that reliable reanalyses can be obtained of earlier periods, where only sparse data are available, using only surface pressure observations where standard corrections are known, when combined with more advanced data assimilation methods. Compo et al. (2006), highlighted that compared to other assimilation methods, using an ensemble Kalman filter provides results which not only cover large scale features, but also many synoptic features and had a smaller analysis error when observations are sparse. For the northern hemisphere extratropics (20°N-90°N) in the upper troposphere, the zonal and meridional wind components have an error and anomaly correlation skill at a level of 0.8 or above from 1895 onwards, for both summer and winter. The summer analysis errors are, however, larger than in winter, which was also identified by Ferguson and Villarini (2014).

Utilising only surface pressure reports to compile the dataset can help overcome issues from differing conventional observations (Pawson and Fiorino, 1999). For example Archer and Caldeira (2008) used the ERA-40 and NCEP/NCAR datasets but only for the period from 1979 when satellite observations were available due to the differences seen in the dataset once satellite observations were introduced. Woollings et al. (2014) has, however, compared North Atlantic Jet latitude and speed from the NCEP-NCAR reanalysis and found "extremely good agreement", for the period from 1948, with the 20CR data.

3. Methodology

Jet streams are diverse in nature and can vary spatially and temporally, which has led to different definitions being used and may possibly lead to the inconsistencies in the results outlined in the introduction. The main approaches adopted to define the jet stream are either, the *maximum* wind speed over one or more isobaric levels, or the *average* wind speed over $30ms^{-1}$ across one or more isobaric surfaces. Woollings et al. (2014) used the maximum zonal wind at the 850mb level after establishing that the results were almost identical to averaging over 925 -700mb level. Pena-Ortiz et al. (2013) used the maximum zonal wind above $30ms^{-1}$ and frequency at each longitude across the 400-100mb level. Frequency of the jet over $30ms^{-1}$ was also used by Kuang et al. (2014). Koch et al. (2006), and Strong and Davis (2007) used maximum wind speed above $30ms^{-1}$ and $27ms^{-1}$ respectively. Archer and Caldeira (2008) used the mass weighted monthly wind speed averages of the zonal and meridional components between 400 and 100mb, whilst (Gan and Wu, 2013) used the 300mb meridional wind velocity to define the jet stream. However, even with the more complex approaches adopted, for example by Archer and Caldeira (2008), only a single jet structure was identified for the northern hemisphere; starting over the Canary Islands and ending, after circumnavigating the globe, over England.

In this study a combination of the above approaches has been used. In line with Archer and Caldeira (2008), the absolute wind speed has been based on the zonal and meridional (u and v) wind velocity components, to ensure that meridional excursions in the jet stream paths are well captured.

As absolute wind speeds are being computed from the zonal and meridional components, the absolute wind speeds ($\overline{U}$) are calculated based on each of the ensemble members:

$$\overline{U} = \frac{1}{n}\sum_{i=1}^{n}(u_i^2 + v_i^2)^{0.5} \quad (1)$$

Where, u_i v_i are the zonal and meridional wind components

and n=56 is the number of ensemble members.

As this study is primarily concerned with longer term trends, using only one isobaric level is considered acceptable. Accordingly, the wind components used to define the jet stream are the 6-hourly 250mb meridional and zonal wind velocity, for each of the 56 20CR ensemble members, spanning the 141 year period from 1871 to 2011, at 2° longitude-latitude horizontal resolution (Compo et al., 2011). 250mb is close to where the maximum velocity is observed (Fang and Yang, 2016).

The maximum windspeed was used to define jet latitude and jet speed, in line with the methodology adopted by (Woollings et al., 2014, Woollings et al., 2010). The algorithm used to calculate the jet stream proceeds as follows. First the 250mb 6-hourly zonal and meridional wind velocity for each of the 56 ensemble members for each year were obtained and the average absolute velocity $\overline{U}$ is calculated according to equation 1. The jet speed was defined as the maximum value of $\overline{U}$ at each longitude.

The jet latitude was defined as the latitude of the maximum average absolute wind velocity ($\overline{U}$ maximum), for each longitude. On occasions when the jet is split into two branches, only the strongest is considered.

The regional areas considered in this study are shown in Figure 1, Eurasia (0-120°E), North Pacific (120°E -120°W), North America (120°W-60°W), and North Atlantic (60°W-0°W). 60°W-0°W was used to define the North Atlantic to provide consistency with previous studies of the North Atlantic jet stream which also use this longitude range (Woollings et al., 2014, Woollings et al., 2010).

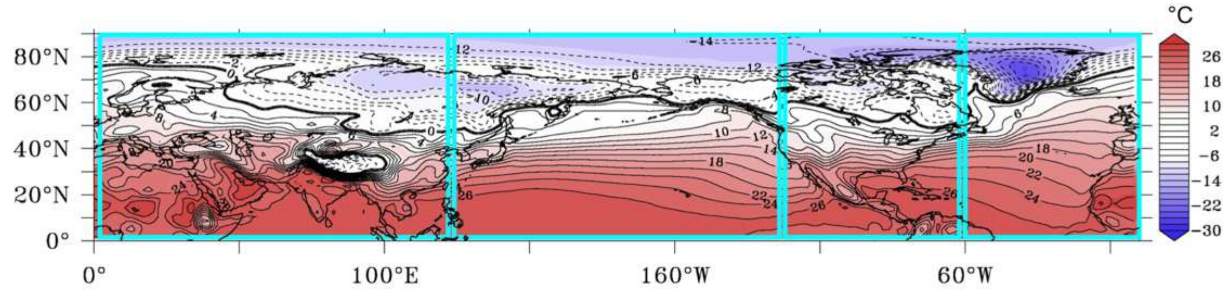

Figure 1 Regional view of the land and ocean areas considered overlaying the annual average 2 m air temperature. Eurasia (0 - 120°E), North Pacific (120°E-120°W), North America (120°W-60°W), and North Atlantic (60°W-0°W)

The ensemble information was used in this study to provide uncertainty estimates. To first establish the robustness of the dataset, and understand the variance of the ensemble members over the 141 year timeframe, 3 separate jet latitude standard deviations were calculated; based on the 6-hourly data, based on the 6-hourly data smoothed over 31 and 91 days using a Parzen filter. The results are illustrated in Figure 2. A seasonal cycle is evident. The standard deviations reach maximum values in summer and minimum values in winter. The range reduces significantly over the period from 1871-2011. The largest variability is where no smoothing has been applied. There is a marked reduction in the jet latitude range during the 1930s to 2° and 1° when the standard deviations are smoothed by applying a low pass filter across the 56 ensemble members over 31 days and 91 days, respectively. Before the 1940s, the standard deviation range is higher across the ensemble members, in all regions, indicating a higher level of uncertainty. This is likely to be caused by insufficient data coverage to constrain the model, and possible statistical inhomogeneity (Ferguson and Villarini, 2014). This effect does need to be incorporated into the interpretation of results, as also highlighted by (Woollings et al., 2014). Accordingly, throughout this study analysis is shown for periods 1871-2011 and 1940-2011, where appropriate. Separate jet speed standard deviations were also calculated on the same basis with similar results (not shown). Importantly, the ensemble spread, is broadly the same across all regions, for the corresponding time period, indicating that all regions can be used for this study.

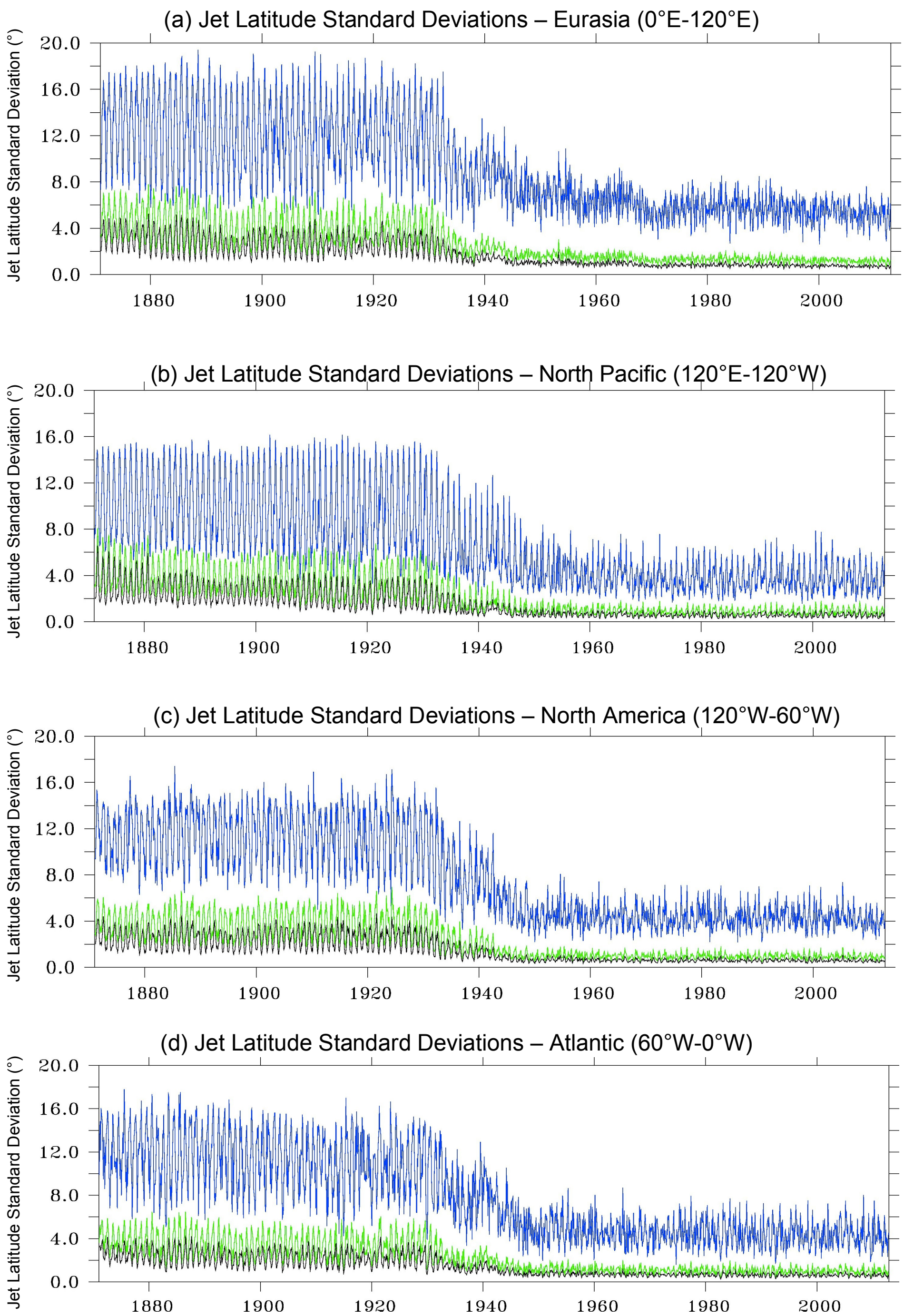

Figure 2 Regional jet latitude standard deviations across the 56 ensemble members from 1871-2011. Blue line - Standard deviation based on the 6-hourly data across the 56 ensemble members. Green line - Standard deviation based on the 6-hourly data smoothed over 31 days by applying a low pass filter across the 56 ensemble members. Black line - Standard deviation based on the 6-hourly data smoothed over 91 days

To assist the analysis and understanding of the jet stream variability, this study also uses air temperature, and geopotential height data. For consistency, data from the 20CR dataset for the period 1871-2011 are used. Air temperature data is obtained from the 2 m air temperature monthly ensemble mean, and tropopause monthly ensemble mean.

Geopotential height data is obtained from the 300mb geopotential height monthly ensemble mean.

4. Results

This section outlines the key findings from this study, first covering the seasonal variation in the jet latitude and speed, highlighting the variations over land masses compared to the ocean basins, before looking at the interannual variability and decadal trends. Where appropriate the results are shown for two periods 1871-2011 and 1940-2011. The latter period is used for comparison, as the spread across the ensemble members is significantly lower after 1940 (Figure 2).

4.1 Seasonal jet latitude and speed climatology

The jet latitude seasonal cycle (Figure 3) shows a poleward shift in summer, but there are regional variations in the amplitude and lag with respect to insolation. For the full analysis period from 1871-2011 (Figure 3a, c, e, and g), the jet latitude amplitude is greatest over land; for Eurasia and North America the range is 20° from 34 - 54°N and 39 - 59°N, respectively. Over the North Atlantic the seasonal range is lower at 10° from 46 - 56°N and over the North Pacific the range is about 15° with a narrow peak in July and August. Only considering the 1940-2011 period (Figure 3b, d, f, and h) we find a reduction in the peak latitude in the summer months by around 3° over land and 2° over the ocean basins. Again, the jet latitude amplitude remains greatest over land; with a maximum for Eurasia of 18° whilst the North Atlantic range is only 7°. There is little difference for the interannual variability between the two periods whereas the uncertainty related to the ensemble spread is much reduced for the 1940-2011 period. The seasonal cycle curves also have different shapes. In all regions there is a response of the jet stream to insolation. Over North America the response of the jet stream broadly follows a sinusoidal curve which lags insolation by about 1-2 months. The peak is broader over Eurasia, particularly for the period 1940-2011. Between February and June, the jet stream moves to its northernmost latitude at around 50°N, it then plateaus at this latitude until October, after which there is a steep decline. The North Atlantic shape is different again and a lag to insolation is evident. There is a broad flat line from January to May with only a 1° increase in latitude. From May onwards there is a 6° increase to September, before a steady fall from September to

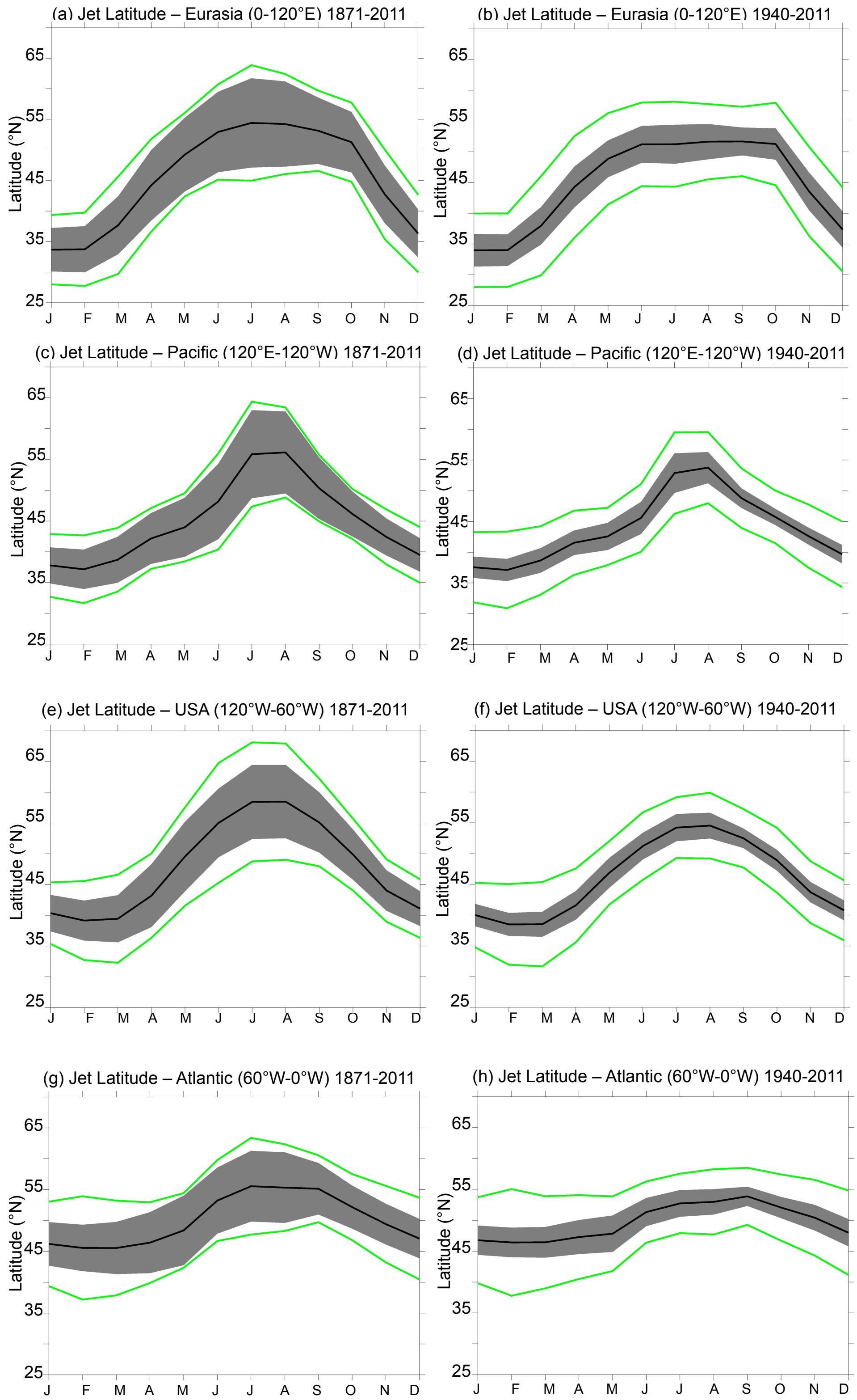

Figure 3 Seasonal Cycle of the Jet Stream Latitude in the Northern Hemisphere by region for periods 1871-2011 (a), (c), (e), (g) and 1940-2011 (b), (d), (f), (h). Black line is mean jet latitude. Grey area is ± 2 standard deviations smoothed over 31 days using a Parzen filter based on the 56 ensemble members. Green line is ±2 standard deviations based on the interannual variability for the period

December. For the 1940-2011 period the seasonal cycle is barely significant and the interannual variability found for any given month largely overlaps with the interannual variability for any of the other months. Over the North Pacific the jet latitude slowly increases from February to June and a narrow peak is reached in July/August which is followed by a steady southward movement from October onwards.

The seasonal cycle of jet speed (Figure 4) shows a similar pattern across land and the North Atlantic and displays a near-sinusoidal curve with maximum wind speeds seen in January around $59ms^{-1}$ and minimum in July around $40ms^{-1}$. The cycle over the North Pacific resembles the inverse cycle seen for jet latitude, with a steep decrease in speed from May to July and steep increase from August to October. Speeds are also highest over the North Pacific, reaching a maximum in January at $66ms^{-1}$ and minimum in July at $38ms^{-1}$. The average jet speed for each region and season is also over $35ms^{-1}$ for each longitude (not shown). The main change observed between the 1871 - 2011 and 1940 -2011 is that in the latter period the summer speeds have decreased by around $3ms^{-1}$ to $39ms^{-1}$, whilst winter speeds have increased across North America and the North Atlantic.

Looking at the seasonal variations across the northern hemisphere (Figure 5) indicates that the zonal variability in jet stream latitude is greatest in the winter months (DJF), resulting in a wave like pattern, with two latitude maxima located over the eastern Pacific and Atlantic. The jet stream follows a well-defined path in winter which is tightly confined, particularly on the western boundary of the North Pacific (33°N) near the Kuroshio current and North Atlantic (41°N) aligning with the Gulf Stream/North Atlantic Current. The jet stream troughs are also located in these areas in winter; the main areas for cyclogenesis. In spring (MAM) and autumn (SON) the jet stream troughs are further north, but remain over the western boundaries of the North Pacific (37°N, 41°N) and North Atlantic (43°N, 47°N) respectively. In summer (JJA) the jet stream follows a more zonal path around 55°N with the main ridge west of Hudson Bay (60°N, 100°W).

Of particular note is the narrow range in the mean jet latitude position in winter along the western boundary of the North Atlantic and North Pacific. The jet is located 1° to the north of the maximum gradient of the 2 m air temperature and is aligned with the temperature contours. The relationship between the mean jet position along the western boundary, and the maximum gradient of 2 m air temperature is retained in Spring and Autumn although not as tightly defined with the mean jet position located 3° and 4° north of the maximum

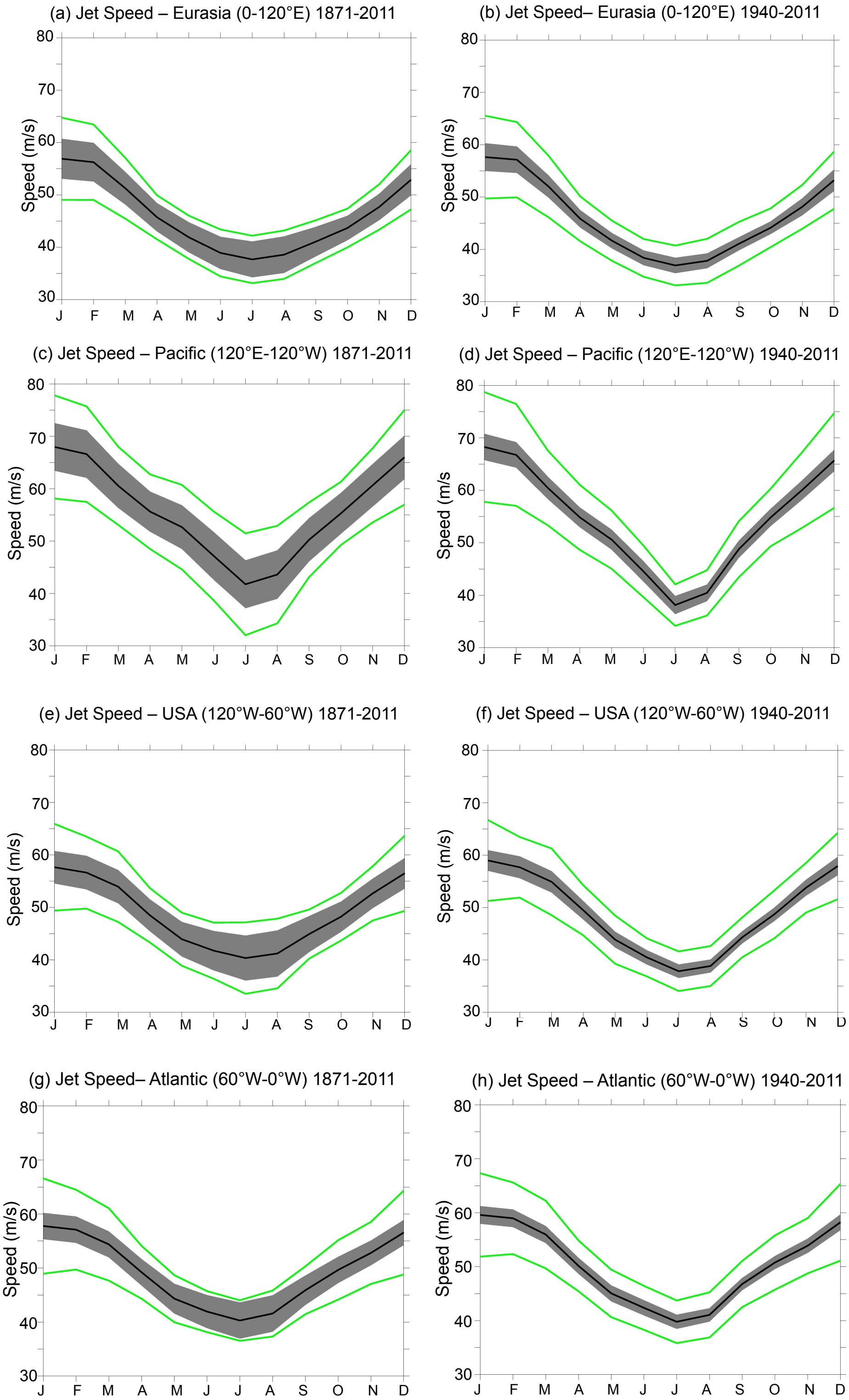

Figure 4 Seasonal Jet Speed Climatology in the Northern Hemisphere by region for periods 1871-2011 (a), (c), (e), (g) and 1940-2011 (b), (d), (f), (h). Black line is mean jet speed. Grey area is ± 2 standard deviations smoothed over 31 days using a Parzen filter based on the 56 ensemble members. Green line is ±2 standard deviations based on the interannual variability for the period

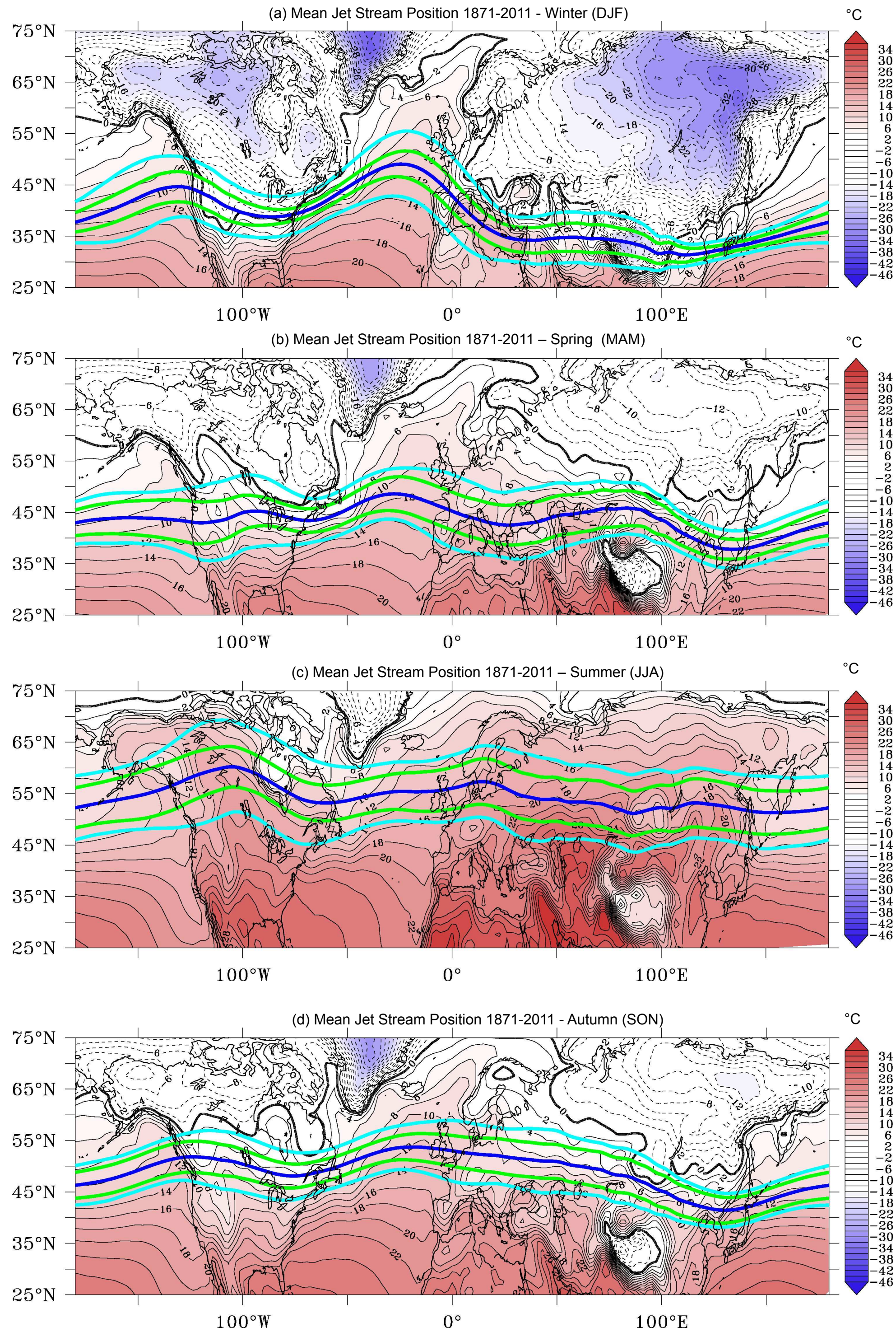

Figure 5 Mean Seasonal Jet Stream Position overlaying the 2 m air temperature for the period 1871 -2011. The dark blue line indicates the mean jet stream position and the green line ± 2 standard deviations of the 6 hourly jet latitude smoothed over 91 days using a Parzen filter, for the period shown, based on the 56 ensemble members. The cyan blue line is ±2 standard deviations of the 6 hourly jet latitude smoothed over 91 days using a Parzen filter, for the period shown, based on the interannual variability for the period. The jet stream overlays the seasonal average 2 m air temperature

gradient, respectively. The 2 m air gradient and land-sea temperature contrast are not as strong in these seasons. No relationship is evident in summer. It would perhaps be expected that the relationship of the maximum gradient of 2 m air temperature and mean jet latitude would also been seen over land. Although there is some relation, it is not as clear.

4.2 Multi-decadal trends in jet latitude and speed

This section details decadal trends for the Northern Hemisphere and then on a regional basis**.** *Significant trends are at the 95% confidence level or higher*. Jet latitude shows differing trends in each season (Figure 6). For the northern hemisphere in winter (DJF) there is a significant 1.2° (0.1°/decade) long-term increase from a mean of 37.5 to 38.7°N (Figure 6). In spring (MAM) there is no significant change in the mean of 44.3°N. In summer (JJA) only the trend after 1940 is considered, due to the range in the standard deviation in the earlier period. There has been a modest 0.3°N increasing trend in jet latitude. In Autumn (SON) there is a significant 1° (0.1°/decade) decrease in the jet latitude from 49.4°N to 48.4°N over 141 years.

When trends are analysed on a regional basis, a different picture unfolds (Figure 7). For winter (DJF) significant increasing trends in jet latitude are seen over the North Atlantic of 3.0°(0.2°/decade) from 44°N to 47°N and over Eurasia with an increase of 1.7°(0.1°/decade) from 33.1°N to 34.8°N. Across the North Pacific and North America there is no change in the mean position over the 141 year period. In Spring (MAM) only the North Atlantic shows a significant increasing trend in mean jet latitude of 1.8° (0.1°/decade) from 45.6 to 47.4°N (Supplementary Figure 1). Over Eurasia there is no change in the mean of 43.6°N. The Pacific and North America show a decreasing trend until the 1940s and increasing thereafter, but the increase is not statistically significant. For the summer (JJA) after 1940, only Eurasia has a significant increase of 1.6° (0.1°/decade) from 51 to 52.6°N (Supplementary Figure 1). The North Atlantic has a modest 0.4° increase. The North Pacific and North America show a 0.3° and 1.2° decrease, respectively, but neither is statistically significant. In Autumn (SON) the North Atlantic is not in line with the hemisphere trend with an increase of 0.8°N, although not statistically significant (Supplementary Figure 1).

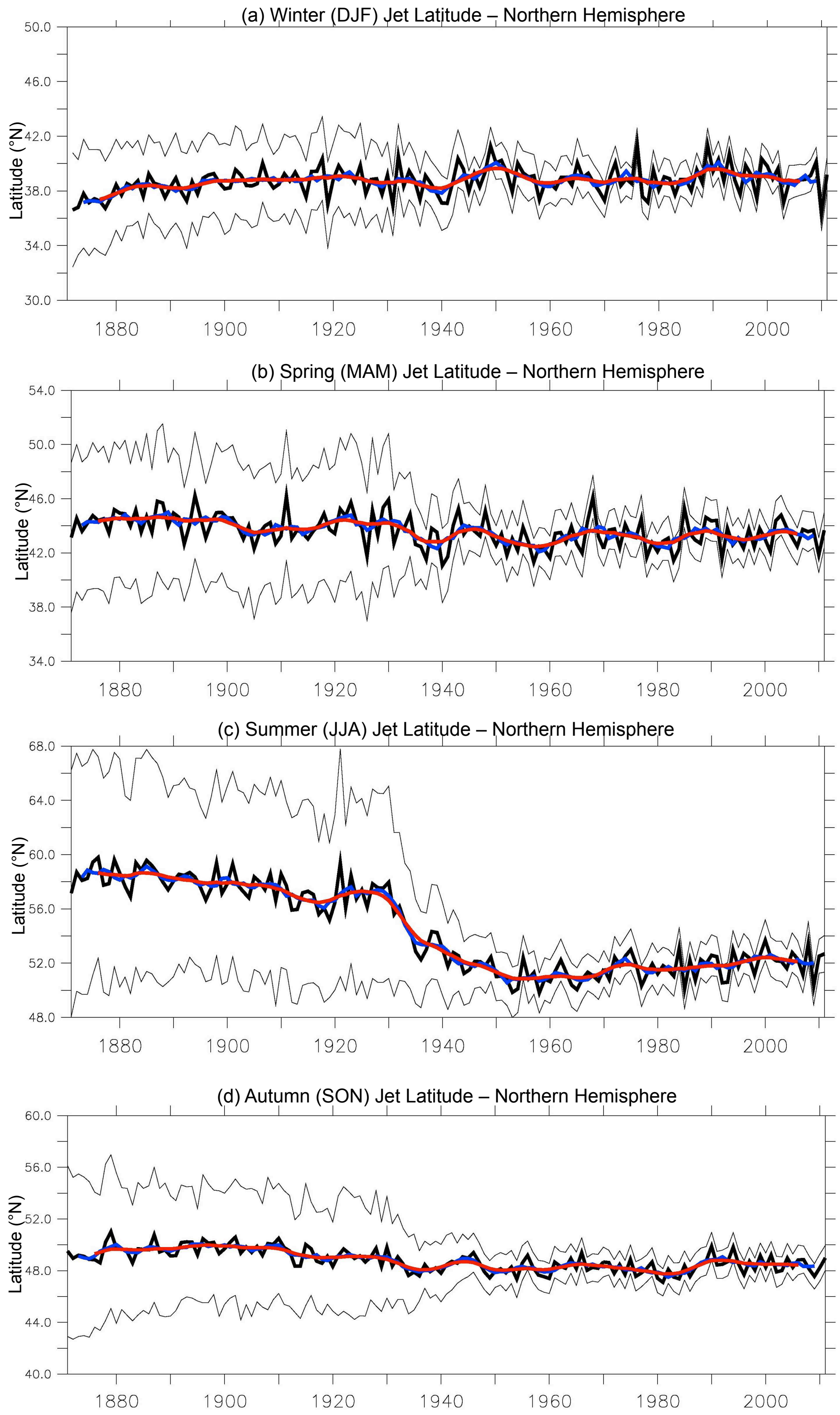

Figure 6 Northern Hemisphere Jet Latitude by season from 1871 -2011. (a)Winter jet latitude (DJF). (b) Spring jet latitude (MAM). (c) Summer jet latitude (JJA). (d) Autumn jet latitude (SON). The thick black line indicates the seasonal mean. The red line indicates the seasonal mean with a Parzen filter smoothing over 11 years. The blue line indicates the 5-year running mean. The thin black lines indicate ±2 standard deviations based on the 6 hourly data for the 56 ensemble members smoothed over 91 days

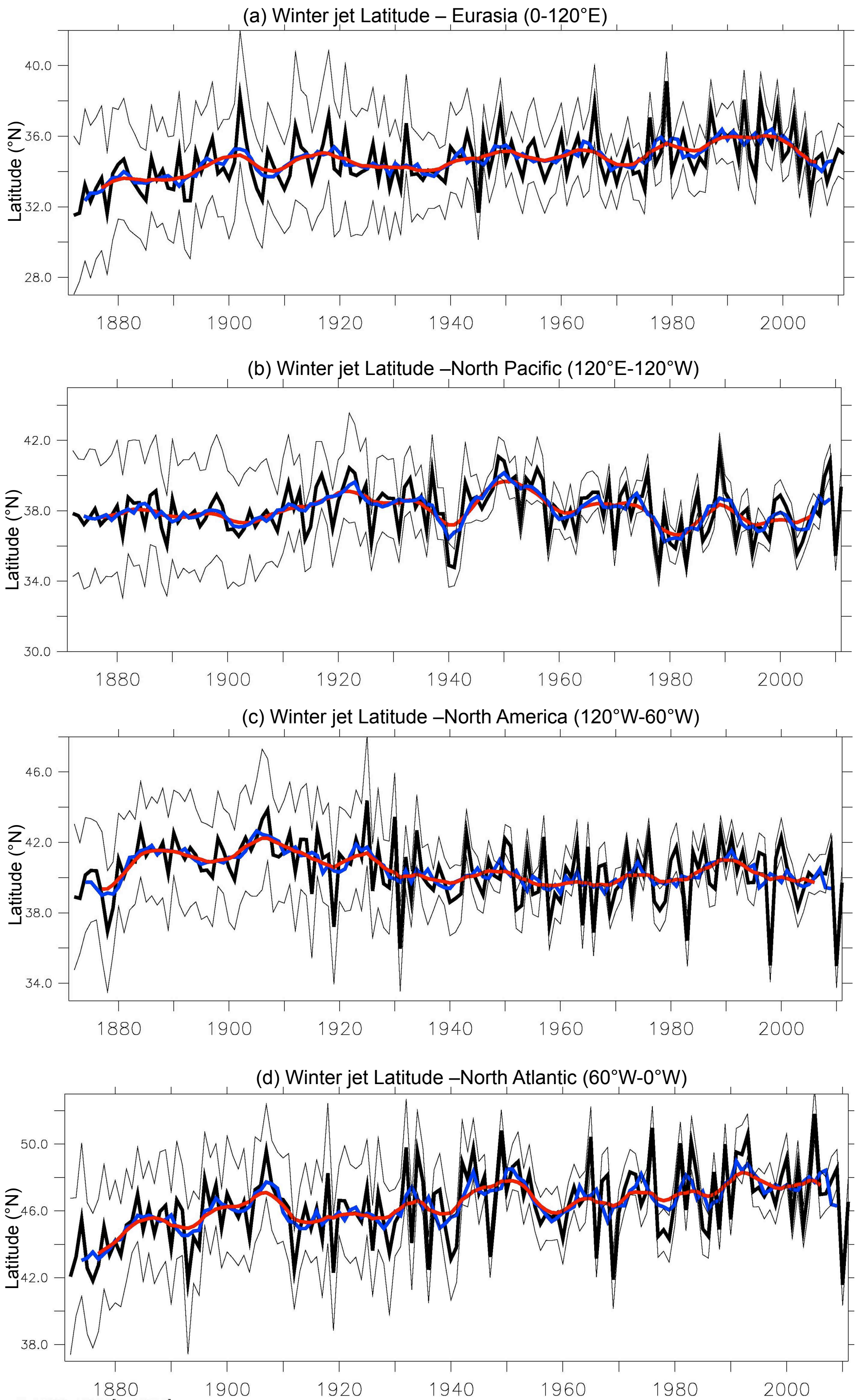

Figure 7 Winter Jet Latitude by region from 1871 -2011. The thick black line indicates the seasonal mean. The red line indicates the seasonal mean with a Parzen filter smoothing over 11 years. The blue line indicates the 5-year running mean. The thin black lines indicate ±2 standard deviations based on the 6 hourly data for the 56 ensemble members smoothed over 91 days

Eurasia has no change, whilst North America and the North Pacific display a significant decreasing trend of 0.15°/decade, however the trend becomes modest after 1940 and is not significant thereafter.

Overall, only the North Atlantic shows an increasing trend in jet latitude across all seasons. Eurasia shows significant increases but only in winter and summer, whilst the North Pacific and North America have either no change or decreases in the seasons.

Jet speed shows a significant increase of 2.0ms^{-1} for winter in the Northern Hemisphere (0.1ms^{-1}/decade) (Figure 8). In the other seasons, there is a decrease in jet speed from 1871-1940 followed by modest (not statistically significant) increase thereafter of between 0.1-0.3ms^{-1}. Again, there are regional differences (Figure 9 and Supplementary Figure 2). In winter, we observe significant jet speed increases: North America 4.73 ms^{-1} (0.3 ms^{-1}/decade), the North Atlantic 4.52 ms^{-1}(0.3 ms^{-1}/decade) and over Eurasia 1.8 ms^{-1}(0.1 ms^{-1}/decade). No trend is seen for the North Pacific. In spring, regional trends are in line with winter, with the largest significant increase seen over the North Atlantic (2.4ms^{-1}, 0.2 ms^{-1}/decade), and weak speed increases of 1ms^{-1} (0.1 ms^{-1}/decade) over North America and Eurasia. In summer, only the period after 1940 is considered. A significant increasing trend is seen over North America of 1.6ms^{-1}(0.2 ms^{-1}/decade). For autumn; the North Atlantic has a significant 3 ms^{-1} (0.2 ms^{-1}/ decade) increase, North America a 1.2 ms^{-1} (0.2 ms^{-1} /decade) increase for the period since 1940, but no change over the full period. Across Eurasia no significant trend is observed. Over the Pacific, the decadal jet speed trends are different. In winter, as with jet latitude, there is no change in the mean jet speed of 67.7ms^{-1} but there is significant interannual variability from 62 to 72 ms^{-1}. In the other seasons, there are no significant trends since the 1940s.

The extent of the relationship between jet latitude and speed was also evaluated for each region and season (Table 1). Over the North Pacific there is a significant negative correlation in all seasons, which is strongest in winter, explaining 42% of the variance. The highest negative correlation is located in the eastern part of the North Pacific at 170°W, explaining

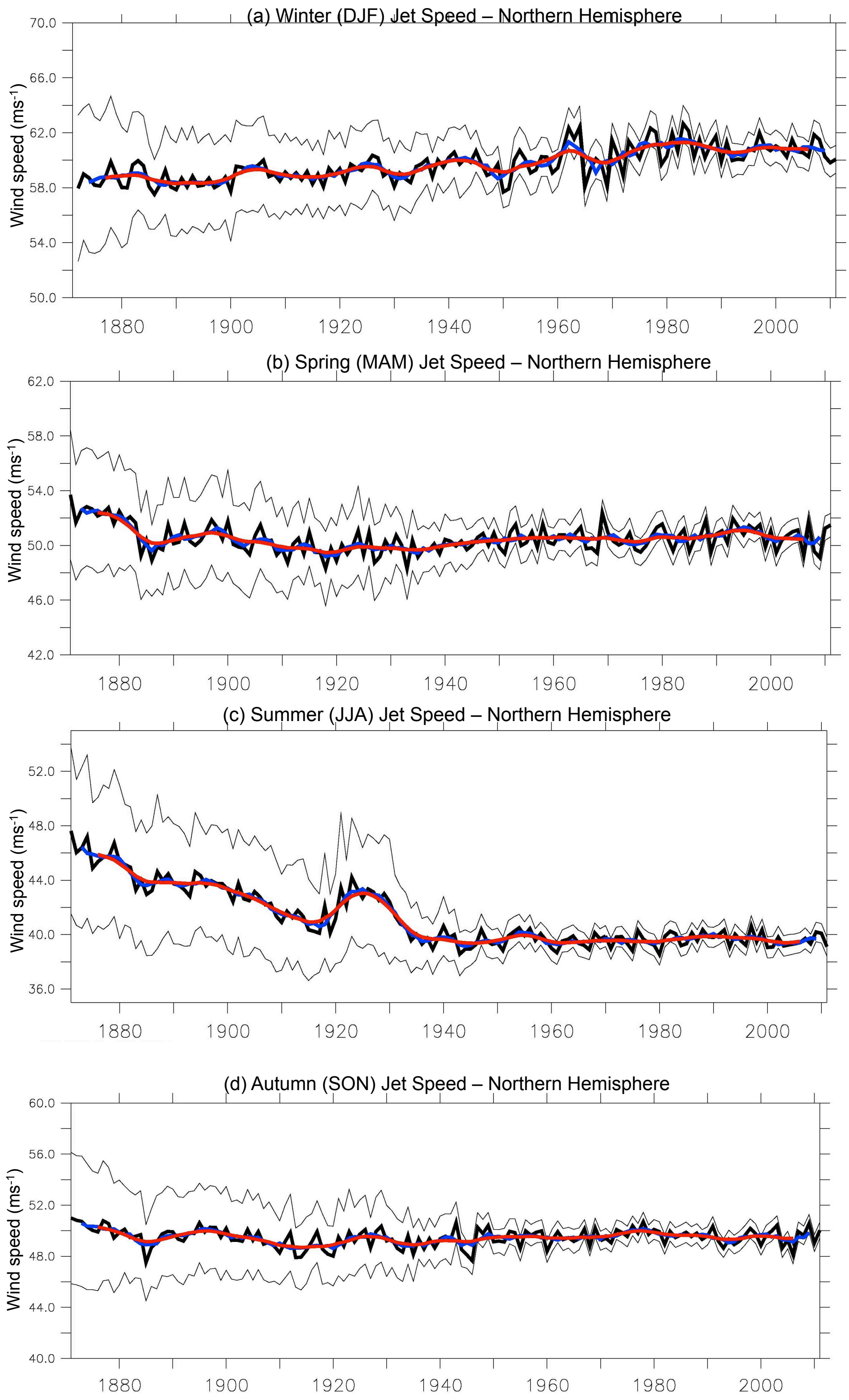

Figure 8 Jet Speed for the Northern Hemisphere from 1871-2011. (a) Winter jet speed (DJF). (b) Spring jet speed (MAM). (c) Summer jet speed (JJA). (d) Autumn jet speed (SON). The thick black line indicates the seasonal mean. The red line indicates the seasonal mean with a Parzen filter smoothing over 11 years. The blue line indicates the 5-year running mean. The thin black lines indicate ±2 standard deviations based on the 6-hourly data for the 56 ensemble members smoothed over 91 days

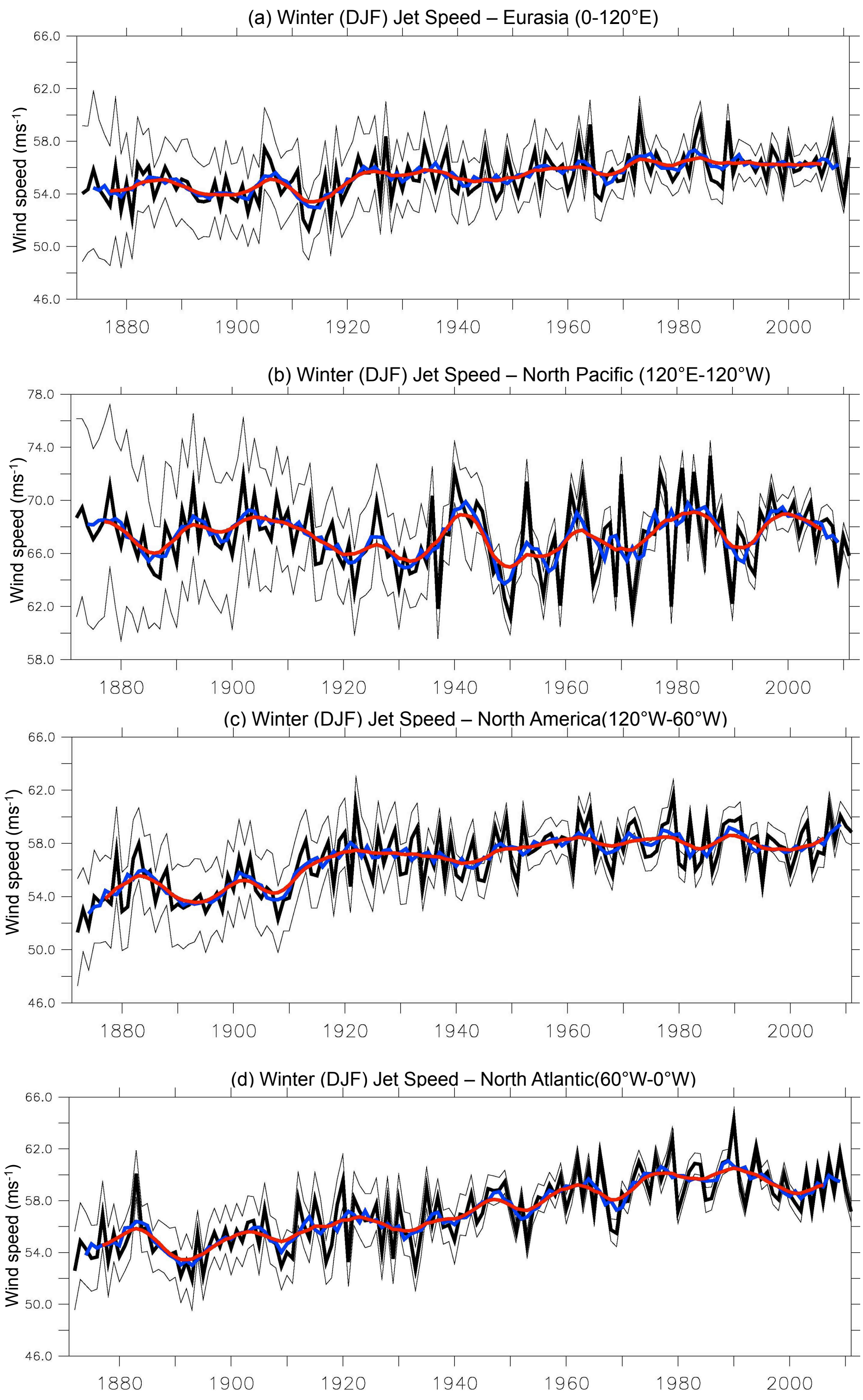

Figure 9 Winter Jet Speed by region from 1871 - 2011. The thick black line indicates the seasonal mean. The red line indicates the seasonal mean with a Parzen filter smoothing over 11 years. The blue line indicates the 5-year running mean. The thin black lines indicate ±2 standard deviations based on the 6-hourly data for the 56 ensemble members smoothed over 91 days

64% of the variance since 1940 (not shown). Over North America, a significant negative correlation exists in spring and autumn. Over the North Atlantic there is a positive correlation in winter and spring, but negative in summer and autumn.

The strongest significant correlation was in winter, for the period 1871-2011, but only explains 9% of the variance. Woollings et al. (2014) also show a low correlation between jet latitude and speed over the North Atlantic. On closer analysis of the North Atlantic in winter, however, there is a negative correlation west of 40°W (maximum value at 60°W r= -0.3) and positive correlation 40°W to 0°W (maximum value at 10°W, r= 0.5), which is masking the true picture for the region. We note that the eastern Atlantic is the only region where significant positive correlations are found between jet stream latitude and speed.

Table 1: Jet Latitude and Jet Speed Correlation (r) for the periods 1940-2011 (1871-2011) Statistically significant correlations at the 95% confidence level or higher are shown in bold

	DJF	**MAM**	**JJA**	**SON**
Eurasia	**-0.24** (-0.08)	0.08 (-0.01)	-0.18 (n/a)	0.06 **(-0.18**)
North Pacific	**-0.65 (-0.65)**	**-0.56** (0.10)	**-0.39** (n/a)	**-0.40** (0.14)
North America	-0.15 (0.15)	**-0.46 (-0.50)**	-0.18 (n/a)	-0.15 **(-0.23)**
North Atlantic	0.02 **(0.30)**	0.16 **(0.24)**	**-0.46** (n/a)	-0.05 **(-0.21)**

4.3 Interannual to decadal variability of jet latitude and speed

The interannual to decadal variability seen in Figures 8 and 9 is analysed in more detail using wavelet analysis and compared to known indices; Atlantic Multidecadal Oscillation (AMO), North Atlantic Oscillation (NAO), Pacific Decadal Oscillation (PDO). The Atlantic Multidecadal Oscillation (AMO) Index, highlights the pattern of SST changes in the North Atlantic and has a period of about 65-70 years (Schlesinger and Ramankutty, 1994). The AMO index (unsmoothed and not detrended) was correlated with the North Atlantic jet latitude. The correlation across all seasons was low at 0.19, in line with the findings by Woollings et al. (2014). The NAO index (Hurrell, 1995) is based on fluctuations in the difference of atmospheric pressure at sea level between the Icelandic Low and the Azores High. The PDO index (Mantua and Hare, 2002) highlights the pattern of SST anomalies in the North Pacific.

We use wavelet cross-coherence to identify the links between jet latitude/ speed and the PDO/NAO (Torrence and Compo, 1998). Correlations between NAO/PDO and jet stream latitude/speed over the Atlantic and Pacific regions are shown in Table 2.

When looking at the PDO/NAO we find that the links with the jet stream latitude and speed vary greatly between regions and seasons. Over the North Pacific, jet latitude and PDO are in antiphase (Table 2 and Figure 10) and in winter show continuous significant coherence for periods between 12 and 30 years. Jet Speed and the PDO are in phase (Table 2 and Figure 11) and in winter show continuous significant coherence between 12 and 26 years.

Table 2: Jet Latitude and Jet Speed Correlation (r) with the NAO/PDO 1940-2011 (1871-2011) Statistically significant correlations at the 95% confidence level or higher are shown in bold

	DJF	**MAM**	**JJA**	**SON**
North Atlantic and NAO				
Latitude	**0.57 (0.45)**	**0.28 (0.30)**	**-0.24** (n/a)	-0.18 **(-0.18)**
Speed	**0.23 (0.18)**	**0.46 (0.44)**	0.15 (n/a)	**0.40 (0.38)**
North Pacific and PDO				
Latitude	**-0.71 (-0.62)**	**-0.51 (-0.44)**	**-0.38** (n/a)	**-0.46 (-0.32)**
Speed	**0.53 (0.45)**	**0.46 (0.42)**	0.16 (n/a)	-0.02 (0.11)

Over the North Atlantic in winter, jet latitude and NAO are in phase and show significant coherence at 20-year timescales for the period 1930-1960 (Figure 10), and significant coherence at 8-10 year timescales for the period since 1980. Jet speed and the NAO are in phase and in spring show significant coherence at 16-24 year timescales for the period since 1940 (Figure 11). Over Eurasia, in the transition seasons of spring and autumn, jet latitude and the NAO show significant coherence since the 1930s on timescales of 16-28 years (Figure 10), whilst jet latitude and the PDO are out of phase over Eurasia and show significant coherence at timescales of 20-28 years (Figure 10). Winter jet speed and the PDO are in phase and show significant coherence at timescales of 28-40 years (Figure 11).

The clearest relations occur over the North Pacific during the winter season. There is a high correlation between jet latitude and jet speed as well as between the jet stream latitude/speed and the Pacific decadal oscillation (PDO) on timescales of about 20 years (Figure 10 and Figure 11). This link is expected as during a positive PDO phase the North Pacific

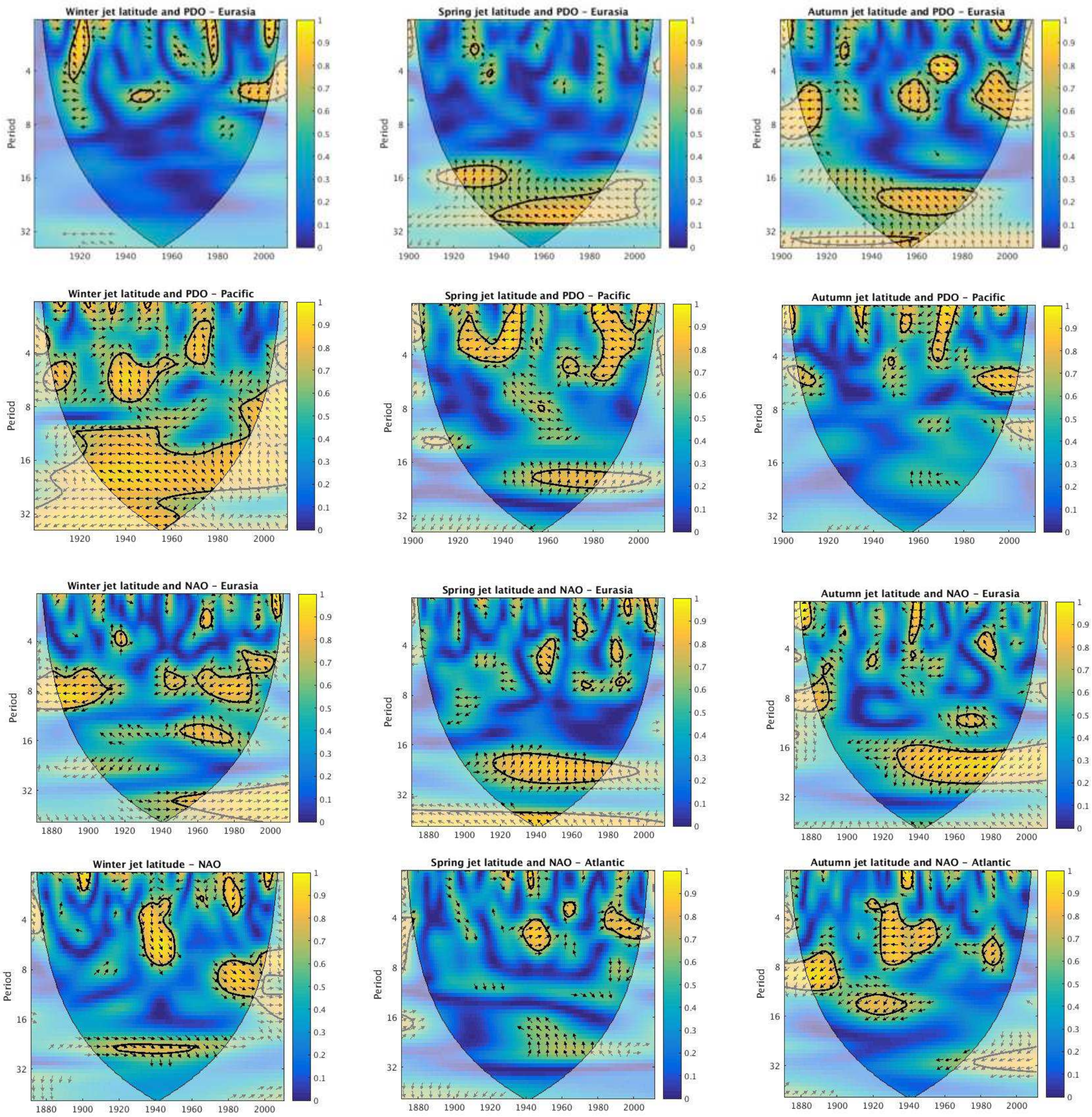

Figure 10 Wavelet coherence for Jet Latitude by region. Colour bar indicates correlation. Black contours indicate statistically significant features (95% confidence level)

is anomalously warm at low latitudes and colder than normal north of the Kuroshio extension (and vice-versa during a negative phase). This indicates that during a positive (negative) PDO phase there is an increased (decreased) meridional temperature gradient which is conducive to stronger winds over the North Pacific region. At the same time the colder than average temperature over the Pacific subpolar gyre region is conducive to a southward shift of the jet stream. This is consistent with the phase relationship between jet stream latitude and speed (Figure 10 and Figure 11) which suggests an out of phase andin-phase relationship respectively. The coherence between the jet latitude/speed and the PDO occurs for periods of about 20 years which are consistent with one of the dominant timescales of the PDO (Mantua and Hare, 2002). The correlation between the PDO and the

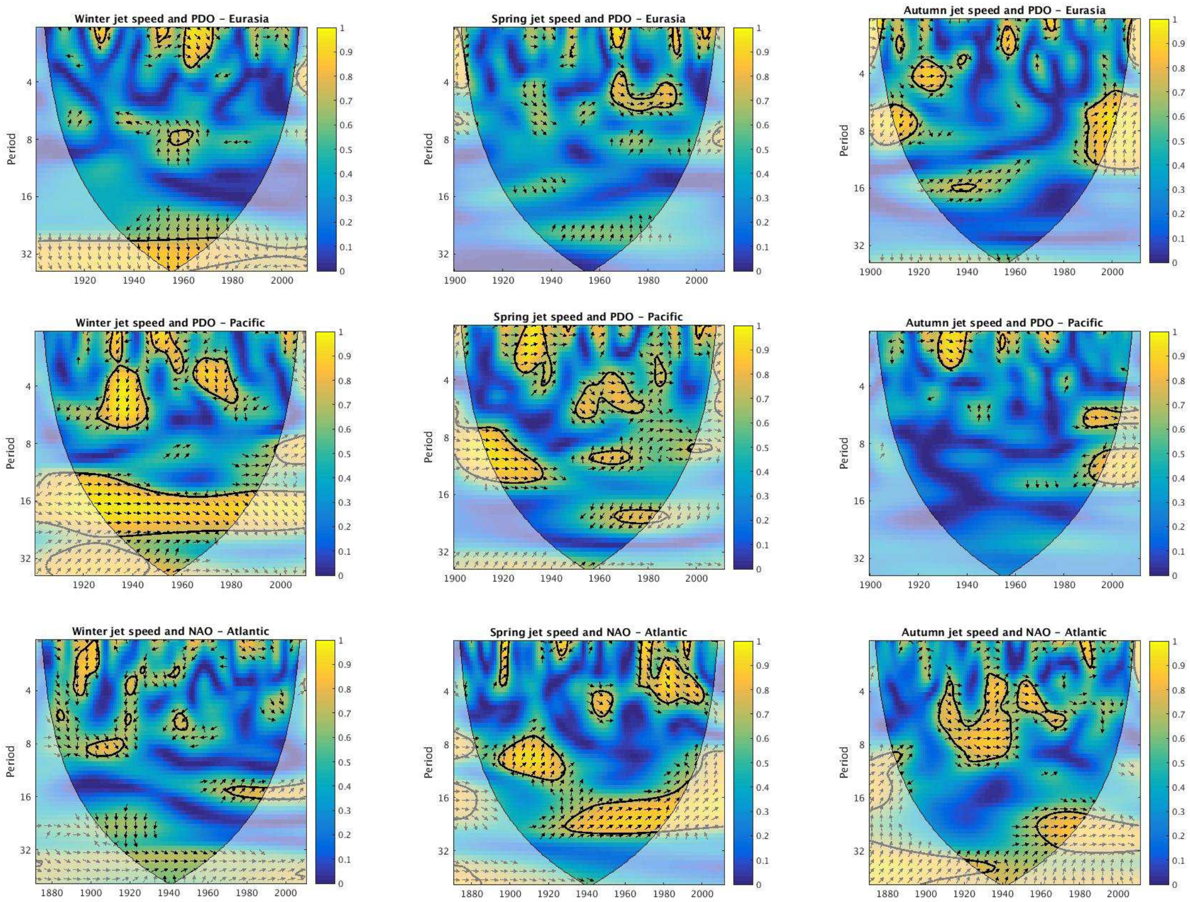

Figure 11 Wavelet coherence for Jet Speed by region. Colour bar indicates correlation. Black contours indicate statistically significant features (95% confidence level)

jet latitude over the Pacific domain is substantially weaker during spring and autumn but over Eurasia we find a significant cross coherence between the PDO and jet latitude (Figure 10), this contrasts with the winter season when the cross-coherence between PDO and the jet latitude and speed is strongest over the Pacific but we find no relationship over Eurasia (Figure 10). This will be further discussed in section 5.3.

5. Discussion

This study highlights that the jet variability, on seasonal to decadal timescales, is different in each region; North Atlantic, North Pacific, Eurasia and North America. Although some similarities exist, the significant differences suggest separate mechanisms are modulating the jet latitude and speed behaviour, which are now discussed in more detail.

5.1 Seasonal Jet Climatology

Over the oceans, particularly the North Atlantic, the annual range in jet latitude is significantly lower. This is linked to the lower variability in the seasonal 2 m air temperature over the oceans, which is due to the greater heat capacity of the oceans of 6 x 10^{24} J K^{-1} compared to the atmosphere of 5 x10^{21} J K^{-1} (Levitus, 1983). The larger oceanic heat capacity results in an accumulation of heat in the mid-latitude oceans during the summer, which is released during the winter months and reduces the overlying temperature range. Compared to North America and Eurasia, the seasonal cycle of the jet latitude is lagged over the North Atlantic and Pacific and the maximum/minimum is reached in September and March, respectively. These findings are similar to Woollings et al. (2014) with a peak maximum latitude in September over the North Atlantic, although Woollings et al. (2014) show a seasonal range in latitude of 5° compared to the 10° (7° for the period 1940-2011) found in this study, perhaps related to the different pressure heights analysed, 850 mb versus 250 mb here. Czaja (2009) found the mean jet stream latitude to be 48°N for the North Atlantic, with a standard deviation of 7° for the period 1980 -2005. It is important that models replicate jet seasonality correctly in order to simulate seasons realistically. Harvey et al. (2020) found that jet stream biases have improved in the CMIP 6 models (compared to CMIP 5) over the Atlantic but still place the jet stream too far south in winter therefore overestimating the seasonal cycle. Little improvement in the biases has been seen over the Pacific where there is an equatorward bias in winter.

The seasonal jet stream range is much smaller over the North Atlantic than over the North Pacific. A key difference between these basins is the poleward meridional heat transport (MHT) by the oceans. In the Atlantic sector the oceanic MHT is positive at all latitudes and there is a net MHT across the equator (Trenberth and Caron, 2001). The Atlantic MHT reaches a maximum of 1.3 PW at 25°N, associated with the Atlantic Meridional Overturning

Circulation (AMOC) (Johns et al., 2011). The oceanic MHT poleward in the Pacific is lower at 0.76PW at 25°N (Bryden et al., 1991) and is predominantly poleward in the Northern and Southern Hemispheres (Trenberth and Caron, 2001). The stronger oceanic MHT in the Atlantic leads to SSTs up to 4°C warmer at similar latitudes in the Atlantic than in the Pacific (Levitus, 1983), and decreases the poleward temperature gradient resulting in a reduced atmospheric MHT, in line with the Bjerknes compensation (van der Swaluw et al., 2007). These results suggest that oceanic MHT changes could impact the seasonal variations in the jet latitude, but further research on this hypothesis would be required to confirm this. The tightly defined winter mean jet stream position across the western boundary of the North Atlantic and North Pacific (Figure 5) in the region where 2 m air temperature and SST gradients are strongest is in line with the studies by O'Reilly and Czaja (2015) for the western Pacific and in the North Atlantic by Feliks et al. (2016), O'Reilly et al. (2016) and Fang and Yang (2016). What is important here is that the findings over shorter periods of time and 850 mb are confirmed in this study over 141 years and at 250mb, and also show the interannual variability over that period.

5.2 Multi-decadal trends in jet latitude and speed

For the Northern hemisphere as a whole, there is a significant 0.1°/decade increase in jet latitude in winter, no significant trend in spring or summer and a significant 0.1°/decade decrease in autumn which is in line with the seasonal findings by Pena-Ortiz et al. (2013) using the same data but their winter and autumn trends were not significant, due to the shorter period analysed.

On a regional basis, however, the long-term trend from 1871-2011 in jet latitude is not uniform. Only the North Atlantic shows an increasing trend across all seasons, with a maximum increase seen in winter of 3.0° (0.2°/decade), which is in agreement with Woollings et al. (2014). Eurasia shows significant increases but only in winter (1.5°, 0.1°/decade), in line with Strong and Davis (2007), and summer (1.6°, 0.1°/decade), where the increase is greater than for the North Atlantic. Over the North Pacific and North America there is either no change or decreases over the seasons, which does not agree with the work of Strong and Davis (2007), who found an increasing trend over the East Pacific between 1958-2007.

It is possible that the differences in regional trends are due to the variation in the uncertainty in the dataset on a regional basis. However, this is unlikely, as it has been accounted for in the interpretation of the results by using data post 1940 for the summer period, and also where the jet latitude trend changes materially after 1940.

Overall, two broad jet latitude patterns have emerged; poleward shifts over the North Atlantic and Eurasia and flat/decreasing trends over the North Pacific and North America. The increasing jet latitude trends seen over the North Atlantic and Eurasia are in line with other northern hemisphere research by Woollings et al. (2014) and Pena-Ortiz et al. (2013), and consistent with a decreasing temperature gradient between the poles and the equator at the tropopause, as highlighted in Figure 12.

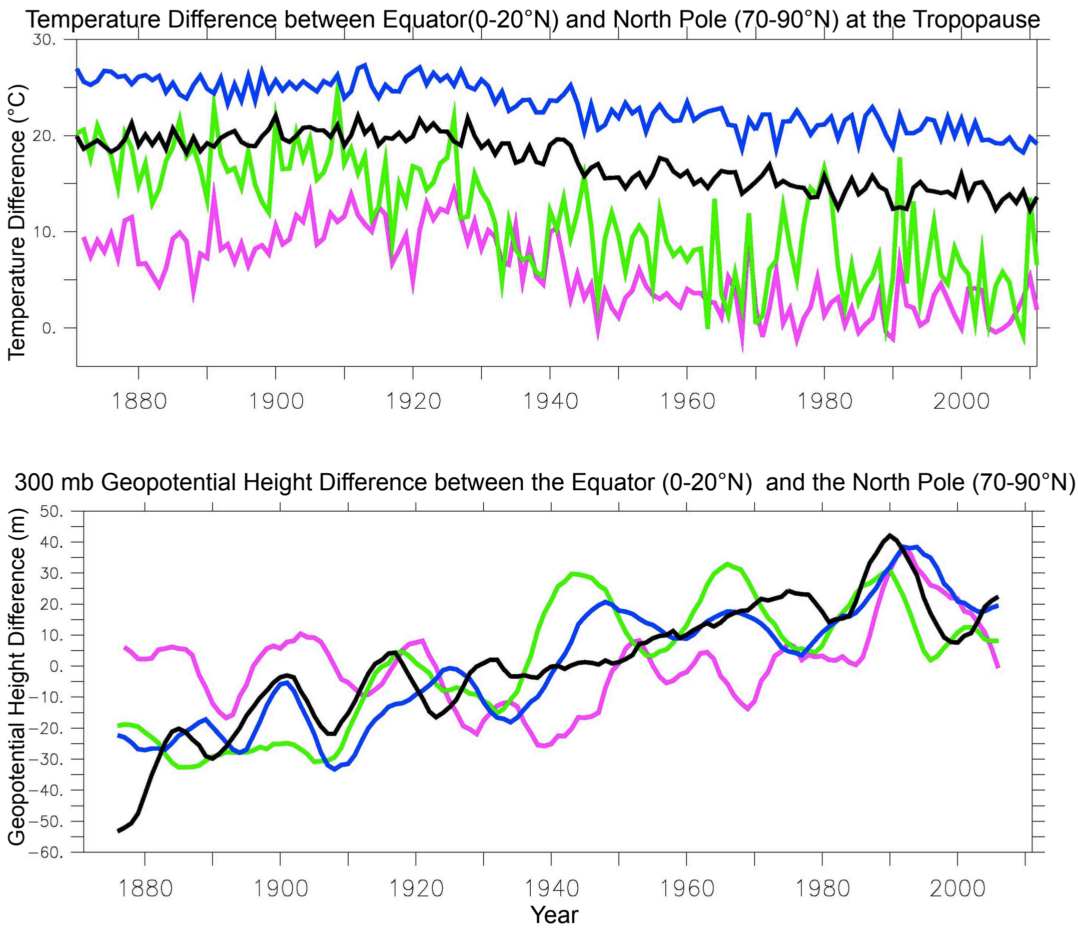

Figure 12 Northern Hemisphere temperature difference at the Tropopause (upper panel) and 300mb Geopotential Height Difference (lower panel) between the equator (0-20°N) and North Pole (70-90°N) for the period 1871-2011. Pink line indicates winter (DJF), Green line spring (MAM), Blue Line summer (JJA), Black line autumn (SON)

On a decadal basis, in line with the seasonal results, it appears that different mechanisms are impacting jet latitude in the North Pacific compared to the North Atlantic. This is consistent with results by Harvey et al. (2014) who found, in the CMIP5 models, that the North Atlantic winter time storm track was sensitive to equator to pole temperature differences, but suggest other mechanisms such as changes to the zonal structure of the Tropical Pacific SSTs may influence the North Pacific storm track. Kuang et al. (2014) also found that the jet variability was sensitive to temperature gradients and baroclinicity over the Atlantic, whereas eddy heat and momentum transport were important over the Pacific.

For the whole northern hemisphere there has been a significant $0.1ms^{-1}$ /decade increase in jet speed in winter, which is lower than the significant findings by Pena-Ortiz et al. (2013) using the NCEP/NCAR data for the shorter period (1958-2008 and 1979-2008). For the other seasons, a decrease was seen from 1871-1940 and very modest increases thereafter, which are not significant. The findings are in agreement with Pena-Ortiz et al. (2013) using the 20CR data, but lower than the increasing trends in speeds seen using NCEP/NCAR data for the shorter period. Archer and Caldeira (2008) found increasing trends in winter and summer for the northern hemisphere.

The regional trends, however, show that increases are seen in winter, spring and autumn in the North Atlantic, Eurasia and North America, many of which are significant and up to $0.3ms^{-1}$/decade in winter. These findings are consistent with the Pena-Ortiz et al. (2013) results using the NCEP/NCAR data.

The North Pacific region shows no change in winter jet speed and decreasing trends in the other seasons. This is not in agreement with Strong and Davis (2007) who find an increasing trend of up to $1.75ms^{-1}$/decade at 35°N between 1958-2007. Archer and Caldeira (2008), however, find negative trends over the Pacific south of the jet core.

The increasing northern hemisphere and regional trends in jet speed are consistent with changes in the 300mb geopotential height gradient between the equator and the North Pole, where there is an increasing trend of up to 50m in each season (Figure 12), which would be expected to lead to an increase in jet speed. The regional exception is over the North Pacific (not shown), where there is a decreasing trend in geopotential height gradient in winter and increasing trend in the other seasons, which is not consistent with the wind speed trends observed.

5.3 Interannual to Decadal Variability

Interannual variability is most evident in the North Pacific, where 50% of the variance in North Pacific winter jet latitude variability and 28% of the winter jet speed variance is explained through the correlation with the PDO index since 1940 (Figure 10, Figure 11 and Table 2). However, overall, there is no consistent link between jet stream latitude and speed or between the jet stream and the NAO and PDO for different regions and seasons. Significant correlations can sometimes be found for some seasons/regions but not for others. An in-depth study of the reasons for the presence (absence) of clear relations is beyond the scope of this study. However, in the following we will illustrate and provide some tentative explanations for the presence or absence of coherence between the jet stream and the PDO/NAO. The link between the PDO and the jet stream is not confined to the Pacific but is also seen over Eurasia Figure 10 and 11. In contrast to the Pacific, the strongest coherence with jet latitude is not found in winter but during spring and autumn. As for the PDO we find significant cross wavelet correlations between the NAO and the jet latitude over Eurasia during spring and autumn for periods of around 20 years but not for winter. Given the large spatial scales of both the PDO and the NAO one could expect these modes of variability to affect the jet stream over Eurasia. So why is this cross correlation not seen during winter when the cross-coherence between jet and PDO (NAO) is strongest over the Pacific (Atlantic)?

For an explanation it is useful to look at the seasonal evolution of the Siberian High (SH) and of the related cold air pool. The SH is the strongest centre of action on the Northern Hemisphere during winter. Most pronounced in winter it is also present – albeit weaker – during spring and autumn and only vanishes in summer (Figure 13). In autumn and spring the SH expands and wanes. The pool of cold air linked to the SH develops from September onwards in Yakutia and the Baikal region from where it gradually spreads westward reaching its full extent in January. The SH is an extremely persistent winter feature around which the jet stream has to swerve. Even though the strength of the SH varies on interannual timescales, this variability is small compared to the average winter SH strength. This is illustrated with the ratio R_i in Figure 13. R_i is a measure of the average strength of surface level pressure features with respect to their interannual variability:

$$R_i = \frac{|\langle SLP_i \rangle - \overline{\langle SLP_i \rangle}|}{\sqrt{\frac{1}{n}\sum_{j=1}^{n}(SLP_{ij} - \langle SLP_i \rangle)^2}}, \quad i = [1,...,12]$$

$$\overline{\langle SLP_i \rangle} = \frac{1}{2\pi}\int_0^{2\pi} \langle SLP_i \rangle d\vartheta,$$

$$\langle SLP_i \rangle = \frac{1}{n}\sum_{j=1}^{n} SLP_{ij}$$

where SLP_{ij} is the sea level pressure for month i in the year j, <> denote the time average for the month i over the 1871-2011 period and the overbar denotes the zonal average (θ is the azimuth).

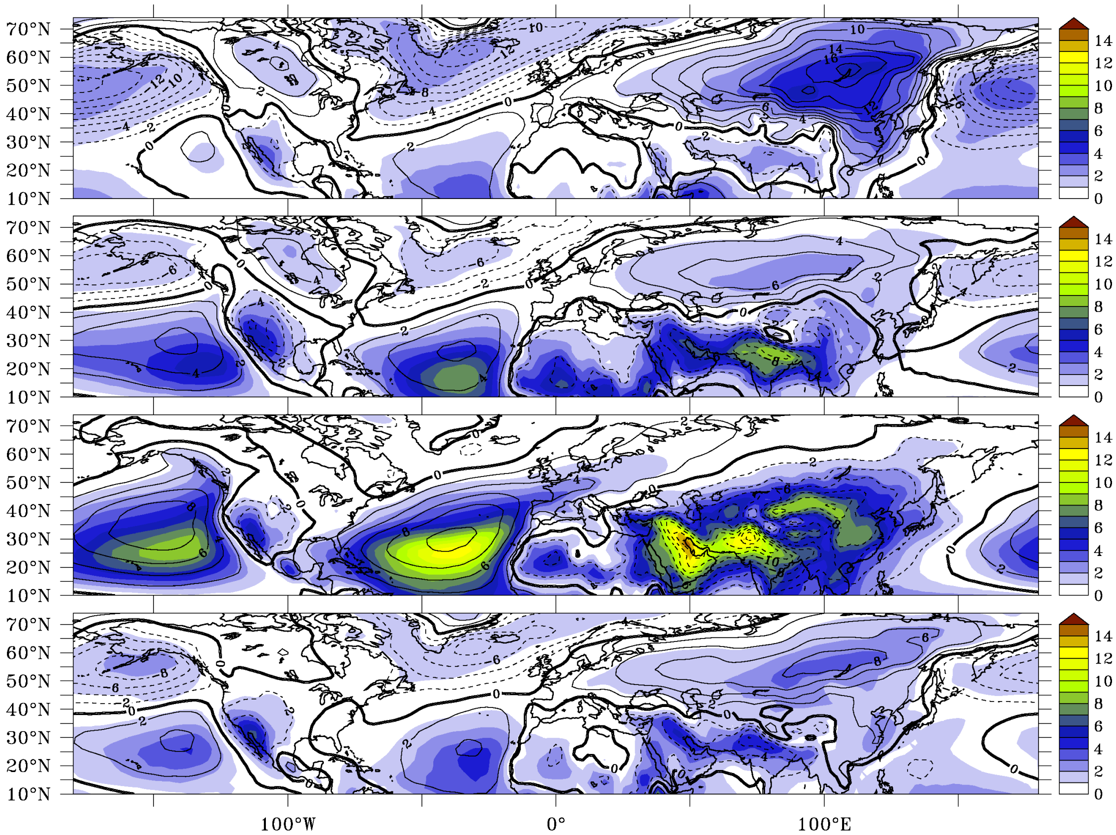

Figure 13 Sea level pressure (SLP) for each season minus the zonally averaged SLP for that season(contours). Shading shows the ratio R_i for DJF, MAM, JJA, SON (from top to bottom). Units are hPa.

During the winter season the highest ratio R_i occurs over eastern Siberia over the south-eastern SH. What the high values of R_i over eastern Siberia in winter suggest is that that even in years when the SH is very weak the pressure over eastern Siberia remains higher than at the adjacent regions further south. With R_i around 5 (Figure 55, top) the SH is more stable than any of the other centres of action of the Northern Hemisphere in winter (Icelandic Low, Aleutian Low, North American High). As the jet stream follows the southern flank of the SH it has to make a southward excursion taking it to the southernmost latitudes of its path around the globe. The stability of the SH is reflected in the jet stream path and Figure 5 shows that nowhere else the jet stream is as tightly confined with by far the lowest temporal (and cross ensemble) variability. The stability of the SH and of the jet stream over East Asia can explain why the cross wavelet correlation seen between the PDO and the jet stream during winter over Eurasia (Figure 10) is so low: no matter what the state of the PDO, NAO or indeed any other atmospheric mode of variability, the SH always dominates the winter pressure pattern over East Asia leading to similar average jet stream paths in most winters. During the transitional seasons of spring and autumn, however, the SH is weaker (albeit still present, see Figure 10 and Figure 13, 2nd and bottom panels) and modes of variability such as the PDO and the NAO start to compete with the SH in terms of influence on the jet stream path. Note that the maximum values of the ratio R_i on the Northern Hemisphere in spring and summer can exceed the winter maxima seen over Siberia. However, these values occur along the south-eastern flanks of the Azores and Pacific Highs as well as over the low pressure area over Southern Asia linked to the Asian Monsoon. All these features are located well south of the jet stream position for these seasons (Figure 5) and hence do not constrain the jet stream path like the SH in winter.

6. Conclusions

For jet latitude and speed, this study has shown the 20CR dataset to be robust, and for winter (DJF), spring (MAM) and autumn (SON) there are no apparent spurious discontinuities or drifts in all regions for the 1871-2011 period. The summer (JJA) only appears robust from 1940 onwards. It is also evident that jet latitude and speed studies need to be carried out on a regional basis, rather than for the whole northern hemisphere, as regional trends and magnitudes may cancel out and therefore not be visible when averaged across the whole hemisphere.

The key new findings of this study are that substantial regional differences are seen for jet latitude and speed variability on seasonal to decadal timescales - particularly when comparing land and ocean regions. Seasonally, the ocean acts to reduce the range of seasonal jet latitude variability. This is particularly the case over the North Atlantic, where the oceanic MHT is greatest, and a 10° seasonal latitude range is seen, compared to a 20° range over land. Also, on a seasonal basis, the winter jet variability is more tightly confined over the western boundary of the North Pacific and North Atlantic over the 141-year period. This is the location where the land-sea contrast and SST gradients are strongest.

Interannual to decadal variability in jet latitude and speed is most evident in the North Pacific in winter with continuous significant cross-coherence on timescales of 12-30 years with the PDO, explaining 50% of the variance in winter jet latitude since 1940. A significant cross-coherence for periodicities around 20 years is also found between the PDO and the jet latitude over Eurasia during spring and autumn but not during winter. The absence of any clear link during winter is likely due to the winter strength of the Siberian high which prevents the PDO (or the NAO) from modulating the jet stream position.

Multidecadal trends vary significantly on a regional basis and looking at the Northern Hemisphere as a whole masks the regional difference. This has implications for understanding how the climate will change on a regional basis. Importantly the trends in the North Atlantic are different to the North Pacific. In the North Atlantic increases in jet latitude are seen in all seasons (0.2°/decade in winter). Over Eurasia increases are seen in winter and summer (0.1°/decade), but no increasing trends are seen over the North Pacific and North America. Increases in jet speed are also found in winter, spring and autumn over the North Atlantic, Eurasia and North America. The increasing trends are consistent with the changes in the geopotential height gradients over the period and region. Over the North Pacific no significant change in jet speed has been found in any season after 1940. The differing trends in jet latitude and speed between the North Atlantic and North Pacific, on seasonal to decadal timescales, suggest different mechanisms are operating in these areas.

The jet stream is key to mid-latitude weather and climate and the results suggest different jet stream behaviours and variability on seasonal to decadal timescales for different regions which has implications for models used for climate and weather predictions. To simulate a realistic climate, models would need to be able to reproduce the regional characteristics of the jet stream and interannual variability. An inability to do so (in a statistical sense) would cast doubt on the ability of such a model to generate reliable prediction of regional weather and climate patterns.

References

ANDERSON, J. L., WYMAN, B., ZHANG, S. & HOAR, T. 2005. Assimilation of Surface Pressure Observations Using an Ensemble Filter in an Idealized Global Atmospheric Prediction System. *Journal of the Atmospheric Sciences,* 62, 2925-2938.

ARCHER, C. L. & CALDEIRA, K. 2008. Historical trends in the jet streams. *Geophysical Research Letters,* 35.

BARNES, E. A. & SIMPSON, I. R. 2017. Seasonal Sensitivity of the Northern Hemisphere Jet Streams to Arctic Temperatures on Subseasonal Time Scales. *Journal of Climate,* 30, 10117-10137.

BARRY, R. G. & CHORLEY, R. J. 2009. *Atmosphere, weather and climate,* USA and Canada, Routledge.

BRYDEN, H. L., ROEMMICH, D. H. & CHURCH, J. A. 1991. Ocean heat transport across 24°N in the Pacific. *Deep Sea Research Part A. Oceanographic Research Papers,* 38, 297-324.

COMPO, G. P., WHITAKER, J. S. & SARDESHMUKH, P. D. 2006. Feasibility of a 100-Year Reanalysis Using Only Surface Pressure Data. *Bulletin of the American Meteorological Society,* 87, 175-190.

COMPO, G. P., WHITAKER, J. S., SARDESHMUKH, P. D., MATSUI, N., ALLAN, R. J., YIN, X., GLEASON, B. E., VOSE, R. S., RUTLEDGE, G., BESSEMOULIN, P., BRÖNNIMANN, S., BRUNET, M., CROUTHAMEL, R. I., GRANT, A. N., GROISMAN, P. Y., JONES, P. D., KRUK, M. C., KRUGER, A. C., MARSHALL, G. J., MAUGERI, M., MOK, H. Y., NORDLI, Ø., ROSS, T. F., TRIGO, R. M., WANG, X. L., WOODRUFF, S. D. & WORLEY, S. J. 2011. The Twentieth Century Reanalysis Project. *Quarterly Journal of the Royal Meteorological Society,* 137, 1-28.

CZAJA, A. 2009. Atmospheric Control on the Thermohaline Circulation. *Journal of Physical Oceanography,* 39, 234-247.

CZAJA, A. & BLUNT, N. 2011. A new mechanism for ocean–atmosphere coupling in midlatitudes. *Quarterly Journal of the Royal Meteorological Society,* 137, 1095-1101.

FANG, J. & YANG, X.-Q. 2016. Structure and dynamics of decadal anomalies in the wintertime midlatitude North Pacific ocean–atmosphere system. *Climate Dynamics,* 47, 1989-2007.

FELIKS, Y., GHIL, M. & ROBERTSON, A. W. 2011. The Atmospheric Circulation over the North Atlantic as Induced by the SST Field. *Journal of Climate,* 24, 522-542.

FELIKS, Y., ROBERTSON, A. W. & GHIL, M. 2016. Interannual Variability in North Atlantic Weather: Data Analysis and a Quasigeostrophic Model. *Journal of the Atmospheric Sciences,* 73, 3227-3248.

FERGUSON, C. R. & VILLARINI, G. 2014. An evaluation of the statistical homogeneity of the Twentieth Century Reanalysis. *Climate Dynamics,* 42, 2841-2866.

FU, Q. & LIN, P. 2011. Poleward Shift of Subtropical Jets Inferred from Satellite-Observed Lower-Stratospheric Temperatures. *Journal of Climate,* 24, 5597-5603.

GAN, B. & WU, L. 2013. Seasonal and Long-Term Coupling between Wintertime Storm Tracks and Sea Surface Temperature in the North Pacific. *Journal of Climate,* 26, 6123-6136.

GAN, B. & WU, L. 2014. Feedbacks of Sea Surface Temperature to Wintertime Storm Tracks in the North Atlantic. *Journal of Climate,* 28, 306-323.

HARTMANN, D., KLEIN TANK, A., RUSTICUCCI, M., ALEXANDER, L., BRÖNNIMANN, S., CHARABI, Y., DENTENER, F., DLUGOKENCKY, E., EASTERLING, D., KAPLAN, A., SODEN, B., THORNE, P., WILD, M. & ZHAI, P. 2013. *Observations: Atmosphere and surface. in Climate Change 2013 the Physical Science Basis: Working Group I Contribution to the Fifth Assessment Report of the Intergovernmental Panel on Climate Change.*, Cambridge University Press.

HARVEY, B. J., COOK, P., SHAFFREY, L. C. & SCHIEMANN, R. 2020. The Response of the Northern Hemisphere Storm Tracks and Jet Streams to Climate Change in the CMIP3, CMIP5, and CMIP6 Climate Models. *Journal of Geophysical Research: Atmospheres,* 125**,** e2020JD032701.

HARVEY, B. J., SHAFFREY, L. C. & WOOLLINGS, T. J. 2014. Equator-to-pole temperature differences and the extra-tropical storm track responses of the CMIP5 climate models. *Climate Dynamics,* 43**,** 1171-1182.

HOLTON, J. R. 1992. *An Introduction to Dynamic Meteorology 3rd ed. International Geophysics Series, Vol.23*, Academic Press 511 pp.

HOSKINS, B. J. & VALDES, P. J. 1989. On the Existence of Storm-Tracks. *Journal of the Atmospheric Sciences,* 47**,** 1854-1864.

HURRELL, J. W. 1995. Decadal Trends in the North Atlantic Oscillation: Regional Temperatures and Precipitation. *Science,* 269**,** 676.

IQBAL, W., LEUNG, W.-N. & HANNACHI, A. 2018. Analysis of the variability of the North Atlantic eddy-driven jet stream in CMIP5. *Climate Dynamics,* 51**,** 235-247.

JOHNS, W. E., BARINGER, M. O., BEAL, L. M., CUNNINGHAM, S. A., KANZOW, T., BRYDEN, H. L., HIRSCHI, J. J. M., MAROTZKE, J., MEINEN, C. S., SHAW, B. & CURRY, R. 2011. Continuous, Array-Based Estimates of Atlantic Ocean Heat Transport at 26.5°N. *Journal of Climate,* 24**,** 2429-2449.

KOCH, P., WERNLI, H. & DAVIES, H. C. 2006. An event-based jet-stream climatology and typology. *International Journal of Climatology,* 26**,** 283-301.

KUANG, X., ZHANG, Y., HUANG, Y. & HUANG, D. 2014. Spatial differences in seasonal variation of the upper-tropospheric jet stream in the Northern Hemisphere and its thermal dynamic mechanism. *Theoretical and Applied Climatology,* 117**,** 103-112.

LEVITUS, S. 1983. Climatological Atlas of the World Ocean. *Eos, Transactions American Geophysical Union,* 64**,** 962-963.

MANNEY, G. L. & HEGGLIN, M. I. 2018. Seasonal and Regional Variations of Long-Term Changes in Upper-Tropospheric Jets from Reanalyses. *Journal of Climate,* 31**,** 423-448.

MANTUA, N. J. & HARE, S. R. 2002. The Pacific Decadal Oscillation. *Journal of Oceanography,* 58**,** 35-44.

MINOBE, S., KUWANO-YOSHIDA, A., KOMORI, N., XIE, S.-P. & SMALL, R. J. 2008. Influence of the Gulf Stream on the troposphere. *Nature,* 452**,** 206-209.

NAKAMURA, H., SAMPE, T., TANIMOTO, Y. & SHIMPO, A. 2004. Observed associations among storm tracks, jet streams and midlatitude oceanic fronts. *Geophysical Monograph Series.*

O'REILLY, C. H. & CZAJA, A. 2015. The response of the Pacific storm track and atmospheric circulation to Kuroshio Extension variability. *Quarterly Journal of the Royal Meteorological Society,* 141**,** 52-66.

O'REILLY, C. H., MINOBE, S. & KUWANO-YOSHIDA, A. 2016. The influence of the Gulf Stream on wintertime European blocking. *Climate Dynamics,* 47**,** 1545-1567.

PAWSON, S. & FIORINO, M. 1999. A comparison of reanalyses in the tropical stratosphere. Part 3: inclusion of the pre-satellite data era. *Climate Dynamics,* 15**,** 241-250.

PENA-ORTIZ, C., GALLEGO, D., RIBERA, P., ORDONEZ, P. & ALVAREZ-CASTRO, M. D. C. 2013. Observed trends in the global jet stream characteristics during the second half of the 20th century. *Journal of Geophysical Research: Atmospheres,* 118**,** 2702-2713.

RONALDS, B., BARNES, E. & HASSANZADEH, P. 2018. A Barotropic Mechanism for the Response of Jet Stream Variability to Arctic Amplification and Sea Ice Loss. *Journal of Climate,* 31**,** 7069-7085.

SCHLESINGER, M. E. & RAMANKUTTY, N. 1994. An oscillation in the global climate system of period 65–70 years. *Nature,* 367**,** 723-726.

SHELDON, L. & CZAJA, A. 2014. Seasonal and interannual variability of an index of deep atmospheric convection over western boundary currents. *Quarterly Journal of the Royal Meteorological Society,* 140**,** 22-30.

SIMPSON, I. R., YEAGER, S. G., MCKINNON, K. A. & DESER, C. 2019. Decadal predictability of late winter precipitation in western Europe through an ocean–jet stream connection. *Nature Geoscience,* 12**,** 613-619.

SMALL, R. J., TOMAS, R. A. & BRYAN, F. O. 2014. Storm track response to ocean fronts in a global high-resolution climate model. *Climate Dynamics,* 43**,** 805-828.

SPENSBERGER, C. & SPENGLER, T. 2020. Feature-Based Jet Variability in the Upper Troposphere. *Journal of Climate,* 33**,** 6849-6871.

STRONG, C. & DAVIS, R. E. 2007. Winter jet stream trends over the Northern Hemisphere. *Quarterly Journal of the Royal Meteorological Society,* 133**,** 2109-2115.

TORRENCE, C. & COMPO, G. P. 1998. A Practical Guide to Wavelet Analysis. *Bulletin of the American Meteorological Society,* 79**,** 61-78.

TRENBERTH, K. E. & CARON, J. M. 2001. Estimates of Meridional Atmosphere and Ocean Heat Transports. *Journal of Climate,* 14**,** 3433-3443.

TRENBERTH, K. E. & HURRELL, J. W. 1994. Decadal atmosphere-ocean variations in the Pacific. *Climate Dynamics,* 9**,** 303-319.

VAN DER SWALUW, E., DRIJFHOUT, S. S. & HAZELEGER, W. 2007. Bjerknes Compensation at High Northern Latitudes: The Ocean Forcing the Atmosphere. *Journal of Climate,* 20**,** 6023-6032.

WHITAKER, J. S., COMPO, G. P., WEI, X. & HAMILL, T. M. 2004. Reanalysis without Radiosondes Using Ensemble Data Assimilation. *Monthly Weather Review,* 132**,** 1190-1200.

WOOLLINGS, T., CZUCHNICKI, C. & FRANZKE, C. 2014. Twentieth century North Atlantic jet variability. *Quarterly Journal of the Royal Meteorological Society,* 140**,** 783-791.

WOOLLINGS, T., FRANZKE, C., HODSON, D. L. R., DONG, B., BARNES, E. A., RAIBLE, C. C. & PINTO, J. G. 2015. Contrasting interannual and multidecadal NAO variability. *Climate Dynamics,* 45**,** 539-556.

WOOLLINGS, T., HANNACHI, A. & HOSKINS, B. 2010. Variability of the North Atlantic eddy-driven jet stream. *Quarterly Journal of the Royal Meteorological Society,* 136**,** 856-868.

Acknowledgements

This project was supported by the Natural Environmental Research Council (NERC) [grant number NE/L002531/1] and by the support of the Marine Institute and funded by the Irish Government under the 2019 JPI Climate and JPI Oceans Joint Call (Grant-Aid Agreement No. PBA/CC/20/01). The study was also supported by the UK-China Research and Innovation Partnership Fund through the Met Office Climate Science for Service Partnership (CSSP) China as part of the Newton Fund, the NERC programme North Atlantic Climate System: Integrated Study (ACSIS) (NE/N018044/1), and the NERC project ODYSEA (grant number: NE/M006107/1).

Support for the Twentieth Century Reanalysis Project dataset is provided by the U.S. Department of Energy, Office of Science Innovative and Novel Computational Impact on Theory and Experiment (DOE INCITE) program, and Office of Biological and Environmental Research (BER), and by the National Oceanic and Atmospheric Administration Climate Program Office.

Data availability

Twentieth Century Reanalysis Project every-member data was obtained from the National Energy Research Scientific Computing Centre. (http://portal.nersc.gov/pydap/20C_Reanalysis_ensemble/analysis/)

Wavelet software was provided by C. Torrence and G. Compo, and is available at URL: http://paos.colorado.edu/research/wavelets.

Declarations

The authors declare no competing interests

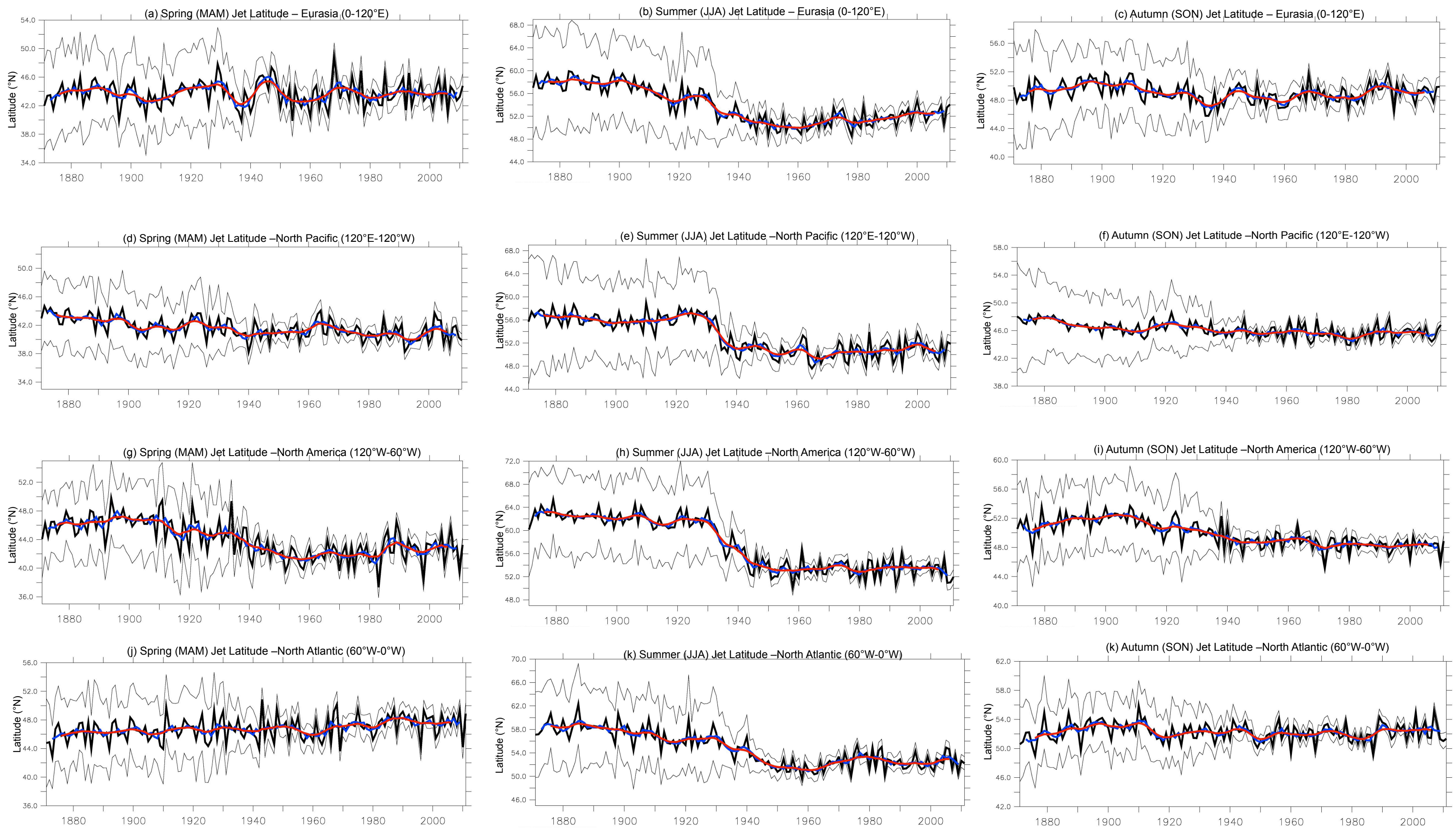

Supplementary Figure 1 Jet Latitude by region and season. Spring (a, d, g, j), Summer (b, e, h, k), Autumn (c, f, I, k) Jet Latitude Decadal Trend by region. The thick black line indicates the seasonal mean. The red line indicates the seasonal mean with a Parzen filter smoothing over 11 years. The blue line indicates the 5-year running mean. The thin black lines indicate ±2 standard deviations based on the 6 hourly data for the 56 ensemble members smoothed over 91 days

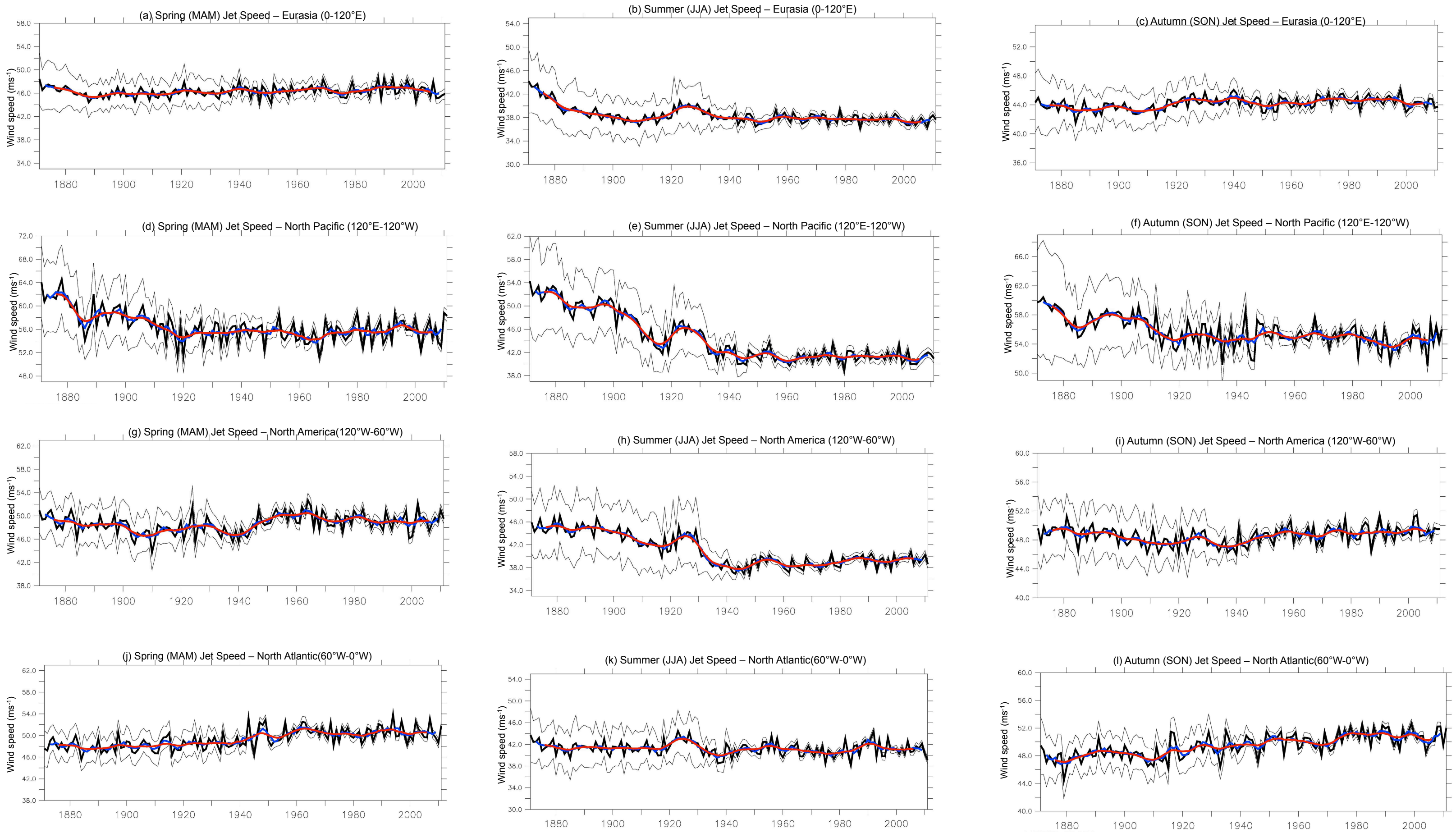

Supplementary Figure 2 Spring (a, d, g, j), Summer (b, e, h, k), Autumn (c, f, I, k) Jet Speed Decadal Trend by region. The thick black line indicates the seasonal mean. The red line indicates the seasonal mean with a Parzen filter smoothing over 11 years. The blue line indicates the 5-year running mean. The thin black lines indicate ±2 standard deviations based on the 6 hourly data for the 56 ensemble members smoothed over 91 days